13th IEA Heat Pump Conference 2020

13th IEA Heat Pump Conference
April 26-29, 2021 Jeju, Korea

Simulation-Based Eco-Economic Assessment Of Heat Pump Systems For Refurbishing All-Electric Non-Residential office building With Complex Energy Demand Structures

Laura Maier*[a], Xuchao Ying[a], Konstantin Finkbeiner[a], Sarah Henn[a], Jan Richarz[a], Markus Nürenberg[a], Tanja Osterhage[a], Dirk Müller[a]

[a] RWTH Aachen University, E.ON Energy Research Center, Institute for Energy Efficient Buildings and Indoor Climate, Mathieustrasse 10, 52074 Aachen

Abstract

Heat pumps (HP) are a key technology to reduce CO_2 emissions in buildings. Yet, profitability of HP-based systems is often poor due to high electricity prices compared to gas prices. Consequently, HP-based systems in new non-residential buildings in Germany only accounted for 17 % in 2018 [1]. However, the German government intends to introduce carbon pricing which could increase HPs´ market penetration.
To evaluate the profitability of all-electric systems in non-residential buildings, the energy system of an old military hospital, which is transformed into a technology and laboratory center called FUBIC, is designed.
We create the building model and analyze the building´s thermal demand using Modelica. Based on this, a HP-based all-electric and a conventional supply scenario are modelled. As KPI, we calculate the annuity and CO_2 emissions in both 2018 and 2030 based on three carbon pricing scenarios.
Results show that, despite its lower emissions, HP-based system´s annuity is lower than that of the conventional scenario regardless of the carbon pricing scenario. The main cost drivers are the demand-related costs which can be decreased by advanced operating strategies.

Selection and/or peer-review under responsibility of the organizers of the 13th IEA Heat Pump Conference 2020.

Keywords: Non-residential Buildings; All-electric Heating Systems; Modelica; Building Stock

1. Motivation

Over the last years, the German government introduced measures in order to reduce CO_2 emissions. These measures mainly focus on the electricity sector representing 21 % of the final energy demand in Germany [2]. Here, the share of renewable energies (RE) in total electricity generation reached 37.8 % in 2018, aiming at 80 % by 2050 [3]. In contrast to that, in the heating and cooling sector, which has a share of 50 % of the final energy demand, RE sources only accounted for 14 % in 2018 [2,4]. Obviously, implementing RE sources in the heating sector would contribute strongly to a decrease in total CO_2 emissions in Germany. This is why the German government set the aim for an almost climate-neutral building stock by 2050 [5]. One measure to achieve this is to substitute fossil-based heat generation systems by those utilizing RE sources [5]. In this context, sector coupling plays a key role. By coupling the electricity and the heating sector, the already realized shift towards REs in the electricity sector can be exploited even more. This is why according to [6] and [7], the electrification of the heating sector is crucial for achieving a holistic energy transition and reach the set aims for 2050. In this study, we refer to heating and cooling systems merely utilizing electricity as energy source as all-electric systems.

* Corresponding author. Tel.: +49-241-80-49795; fax: +49-241-80-49769.
E-mail address: laura.maier@eonerc.rwth-aachen.de.

In the context of all-electric systems, heat pumps (HPs) and chillers are key technologies as they can utilize RE sources (electricity supply and ambient energy) and enable sector coupling. However, in non-residential buildings, the primary energy source is gas and HP-based systems only account for 17 % in new buildings, assuming even lower ratios in the building stock [1]. Nevertheless, non-residential buildings´ share in the total energy demand in the building sector was 37 % in 2014 [8]. This trend is also reflected in the poor amount of current research activities on all-electric systems in the non-residential building sector [9].
A major obstacle to the prevalence of all-electric systems is their profitability. Compared to oil or gas prices, electricity is approximately 4 to 5 times more expensive in Germany [10]. However, fuel prices are strongly fluctuating and their development is uncertain. In addition, there have been some recent developments towards pricing of carbon dioxide, which would strongly influence the given comparison.
This paper contributes to the economic profitability of all-electric systems based on HPs by following steps:

- In chapter 2, an overview of typical energy supply systems in non-residential buildings as well as current and future regulatory boundaries are given.
- We present the developed simulation-based approach for economically and ecologically assessing two supply systems in chapter 3. In addition, future scenarios regarding the development of CO_2 factors and CO_2 pricing are discussed.
- In chapter 4, we show that profitability of HP-based all-electric systems strongly depends on regulatory and economic boundary conditions. Despite their potential to reduce CO_2 emissions, all-electric systems are not necessarily profitable regardless of the carbon pricing scenario applied.
- Based on the results, we deduce a break-even point for CO_2 pricing as well as electricity and gas prices and derive measures in order to support the spread of HP-based all-electric systems.

2. State of the art: Energy supply systems and price development

2.1. Energy supply systems in non-residential buildings

In Germany, the majority of energy systems in non-residential buildings is fossil-based [11]. Besides agriculture, gas is the primarily used energy source. District heating is the second leading source whereas electricity has only small shares. Considering the prediction for the shares of energy sources used for space heating given in [12], we detect a decreasing amount of used gas whilst at the same time increasing renewables such as biomass or geothermal energy. According to the forecast, the absolute consumption of electricity used for space heating remains almost constant between 2009 and 2050 indicating that HPs´ share will remain constant as well.

According to the forecasts presented in [12], electricity will not dominate future heating supply. One reason are high electricity prices in comparison to the other energy prices [10]. This results in the decreased integration of HPs despite their higher efficiency in comparison to conventional heat generators. In addition, HPs have higher capital-related cost when compared to conventional boilers even reinforcing this effect. One aspect which might increase the profitability of HP-based energy systems, however, is the development of carbon pricing. Over the last years, different measures to price CO_2 emissions have been introduced which will greatly influence the profitability of energy systems and thus the choice of energy sources. As HPs support the integration of REs, carbon pricing would encourage their implementation.

2.2. Current and future energy and CO_2 prices

When assessing the profitability of energy systems, regulatory and economic boundary conditions strongly influence the results. The following chapter summarizes current and future energy price developments as well as methods of carbon pricing.
A major reason for the prevalence of gas-based heating systems are low gas prices as well as their well-known technology. Over the last 10 years, gas prices even dropped favoring the integration of gas-based energy systems. In 2018, regular customers (20 – 200 GJ/a) paid 6.08 ct/kWh (all taxes included), whereas industrial customers (100 – 1.000 TJ/a) paid 2.65 ct/kWh including consumption taxes (excluding value added tax (VAT)). Since 2009, an average annual gas price decrease of 0.64 % for regular customers and 2.99 % for industrial customers is observed. [7]
In contrast, increasing prices were recorded for electricity. Prices for the German regular customer (2.5 – 5 MWh/a) have risen by an average of 2.77 % per year over the past ten years. In the large customer segment (2

– 20 GWh/a) the increase was slightly lower at 2.19 % per year. In the second half of 2018, German electricity prices amounted to 12.44 ct/kWh for industry (consumption taxes included, VAT excluded), respectively. [7] Obviously, gas prices are 4 to 5 times lower than electricity prices given the current regulatory and boundary conditions. Therefore, HP-based energy systems would have to reach a SCOP of 4 to 5 in order to achieve equal operating costs which is usually not realistic [13].

Nevertheless, the current regulatory and economic boundary conditions are under constant change. A factor which could strongly influence the given conditions is carbon pricing. Over the last years, various forms of carbon pricing have been introduced as a measure to beat climate change in many countries. There are currently two types of CO_2 pricing systems [14]:

- Direct pricing by applying e.g. taxes
- Indirect pricing by introducing certificate trading [15]

In Europe, the latter is realized by the EU Emissions Trading System (ETS). Sectors which are covered by the system are the energy, industrial and EU-aviation sector. Sectors like the traffic, building, small industry, agriculture and waste sector are referred to as Non-ETS sectors. For these, EU member states set the goal for 2030 to reduce emissions by 38 % compared to 2005. In 2018, however, the German government decided to extent the ETS to the heating and traffic sector. They intent to introduce 3 phases in Germany [16]:

1. From 2021 to 2025: CO_2 certificates are sold for fixed prices starting from 10 €/t in 2021 to 35 €/t in 2025.
2. In 2026: A certificate auctioning system is introduced with prices ranging from 35 to 60 €/t combined with a fixed upper limit for overall emissions.
3. From 2027 onwards: Based on the findings of the former phases, the necessity of upper and lower boundary prices is checked and the system will be adapted accordingly.

In contrast to the implemented trading system in Germany, other countries like Switzerland have introduced a direct pricing system realized by a carbon tax. Starting from 2008, the Swiss government has taxed fossil fuels like gas and oil, gradually adapting the price per ton CO_2 depending the overall emission level.
This development will strongly influence the profitability of all-electric systems in comparison to conventional heating systems and might favor the spread of HP-based energy systems.

3. Methodology

In order to economically assess HP-based systems in the non-residential building sectors, a simulation-based approach is adopted to compare two supply scenarios for the refurbishment process of an office and laboratory building called FUBIC. One scenario represents a state-of-the-art set up based on a condensing gas boiler (CGB) whilst the other scenario is a HP-based all-electricity scenario and thus is not common in non-residential buildings.

3.1. Simulation-based assessment of FUBIC

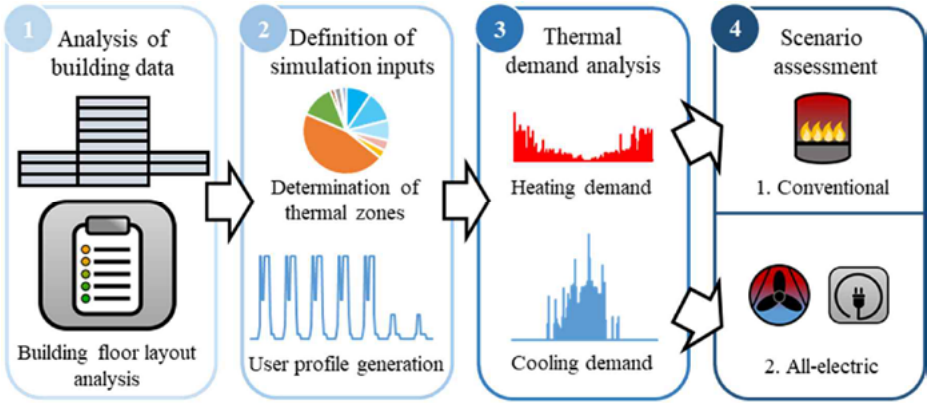

Fig. 1. Simulation-based assessment of a conventional and a HP-based all-electric supply scenario.

The use case is a former military hospital in Berlin, which is transformed into a business, laboratory and innovation center called FUBIC. The center will host start-ups and young companies of the sectors life science, health, communication and IT. FUBIC´s area will be divided into 30 % laboratory spaces, 60 % office spaces and 10 % ancillary areas.

In an early planning phase within the construction process of a building, the operating costs have to be estimated. In practice, this is usually done by applying static calculation methods. However, once the building operation starts, it becomes obvious that a priori estimated energy demand and actual energy consumption often differ greatly [13]. This is especially true for HP-based systems. HPs' efficiency strongly depends on external boundary conditions such as supply and ambient temperatures impeding the prior estimation of energy consumption and thus operating costs.
In this context, dynamic simulations are a promising tool to overcome this obstacle. Dynamic models enable a more realistic assessment of building and energy system performance and behavior. In order to compare the two supply scenarios described before, the two energy systems are implemented in the modelling language Modelica. The used models derive from either the Modelica Standard Library or the AixLib [16]. In this way, we can depict the physically implied dynamics.

In this study, we apply a 4-step approach (s. figure 1). In a first step, we analyze FUBIC´s floor layout deducing zones with similar utilization and boundary conditions (e.g. laboratories, group office, etc.). As a result, we obtain 9 zones which are the basis of the following energetic analysis. For each of these zones, we estimate people presence influencing the use of lights and other electrical devices based on weekly profiles from the Swiss standard SIA 2024 [17]. These boundary conditions serve as inputs for the simulation program and result in both an electrical and a thermal demand in step 3. In the final step, these demands are covered by the supply scenarios. Finally, we can estimate the annuity as well as CO_2 emissions based on the resulting energy demand and maximum thermal loads of the whole system.

3.1.1. Step 1 to 3: FUBIC´s thermal demand
A building model representing the demand side is the first model to be used for the simulation of a building energy system (s. figure 1). It considers various usage purposes of areas inside FUBIC. For modeling such a large multi-zone building, considering various usage purposes of its areas, a reduced order model approach developed by Lauster et al. [17] is applied. The model, which is available in AixLib [16], joins the building physics based on the German Guideline VDI 6007 [18] and the models for internal gains caused by persons, machines and lighting. As described in the guideline, the thermal response of the building can be calculated by using an electric equivalent model with resistances and capacities. In this way, the computation time is reduced considerably resulting from fewer parameters and equations.

For the parametrization of the electric equivalent model, the open-source software tool TEASER [19] is applied. It is used to calculate the resistances and capacities based on information about the geometry and physical properties of the building. Furthermore, TEASER includes a statistical database of representative building setups und thus enables a quick generation of archetype buildings with little input data. The parameters are exported by TEASER in such a structured format that they can be automatically imported into AixLib [16], with which the building model is set up.
The FUBIC building model is extended from an institute building archetype with laboratories. The input data for this archetype is summarized in table 1.

Table 1. Input parameters for simulation tool TEASER for the FUBIC building: Geometry and physical properties.

Number of floors	6 above-ground floors
Net leased area	11,112 m²
Zone layout	Elongated, h = 1 floor
Construction type, year	Heavy, 2018
Ventilation	Mechanical ventilation

With the information extracted from the floor plans, rooms of an equal or similar usage type are classified into one thermal zone, which is assigned with use conditions based on the German standard DIN V 18599 and SIA 2024 [17,20]. The various use conditions determine features like the room set temperatures, air exchange rates, occupancy profiles, internal gains and others. Figure 2 visualizes the resulting zoning of FUBIC

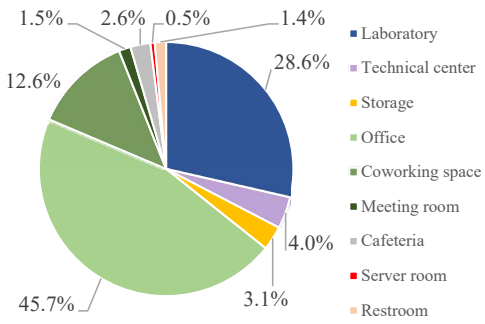

Fig. 2. Classification of FUBIC into thermal zones of equal usage.

The internal gains in the building model include the occupancy of persons, usage of machines and lighting with schedules. The schedules are based on Swiss standard SIA 2024 [17] and are modified for the FUBIC building. For each zone a week profile is defined, considering the difference between weekdays and weekends. The German standard DIN V 18599 [20] also defines the range of indoor comfort temperatures, air exchange rates and conditions of the supply air for each zone. Reference room temperature set points for cooling are given by the German guideline VDI depending on the outdoor temperature to reduce energy demand. [21]
External loads are estimated with weather data given in Test Reference Years (TRY) for Berlin. Germany's National Meteorological Service [22] offers localized weather data of an intermediate TRY as well as special TRYs with a cold winter or a hot summer.
As a simulation result, 4 different thermal demand types are determined in step 3, which are covered by the supply scenarios. The 4 thermal demand types are distinguished as follows:

- Dynamic heating via the ventilation system and static heating via the floor heating system (FHS)
- Dynamic cooling via the ventilation system and additional cooling via recirculation coolers

All in all, 67 % of the heat demand and 22 % of the cooling demand are supplied via the central air handling unit whilst the residual demand is covered by the FHS and the recirculation coolers respectively.

3.1.2. Step 4: Scenario assessment

The main difference between the assessed scenarios is the heat generation system. In the conventional scenario, a CGB is used whilst in the all-electric scenario an air-to-water HP and an electrical backup heater cover FUBIC´s heat demand. The electrical backup heater supports the heat when outdoor temperature drops below a predefined bivalence temperature of -2 °C [23]. Furthermore, the HP is equipped with a modulating compressor (30 to 100 % of design load) as thermal demand is strongly dynamic and thus heat demand can be covered more precisely. In order to guarantee more flexibility, a buffer storage is implemented connecting the HP and the air handling unit (AHU) in parallel. The buffer storage is loaded based on a hysteresis of 5 K while the FHS is controlled by a supply temperature control and a PID controller.
The implemented HP model is taken from the open source library AixLib [16]. It represents a grey box model in which the HP´s COP is based on the Carnot efficiency. The HP´s COP is calculated as follows [16]:

$$COP = \eta_{Carnot} \frac{T_{con}}{(T_{con} - T_{evap})} \quad (1)$$

In equation 1, T_{con} and T_{evap} represent the condenser and evaporator leaving temperatures. The Carnot efficiency η_{Carnot} is assumed to be 50 % and describes the ratio of the HP´s actual COP to the theoretical maximum COP [24]. The implemented model computes transient behaviour using a first order differential relation for the condenser and evaporator water and air volumes. For further information, see documentation of open source model AixLib.Fluid.HeatPumps.Carnot_y [16].

In the given use case, heat has to be supplied at two temperature levels: 50 °C to provide for the AHU´s heat demand and 35 °C for the FHS. These low temperatures support the utilization of HP-based systems, as HP´s COP increases with decreasing supply temperatures (s. equation 1). However, HP´s COP is more significantly influenced by external factors such as the ambient temperature as well as the operating point. In addition, process heating and cooling demand are less flexible demands compared to e.g. space heating. These boundary conditions pose additional requirements for the energy system which is why conventional heat generators are more common in cases like that. Their efficiency does not depend strongly on supply temperatures making prior estimation of energy demands easier. The adopted simulation-based approach, however, enables the detailed analysis of HP´s operation and thus overcomes this obstacle.

3.2. Energy market scenarios

When evaluating the profitability of energy systems, the economic and regulatory boundary conditions strongly influence the outcome. In the following chapter, we analyze important factors that influence the economic assessment of HP-based energy systems focusing on energy prices and CO_2 emissions in Germany.

3.2.1. Development of energy and carbon pricing

Based on the recent development of electricity prices (s. chapter 2.2), a price increase for electricity is assumed for future-related evaluations in this study. Despite the observed decrease in gas prices, the World Energy Outlook New Policies Scenario predicts that gas prices will increase as of 2020 [25]. In the following use case, an increase to 5 ct/kWh for industry (≙ large customers) by 2030 is presumed. Regarding electricity prices, the past trends are extrapolated, resulting in 16 ct/kWh for industrial customers.

Apart from that, carbon prices also influence the economic assessment of energy systems. However, their future development is uncertain as they have just or not yet been introduced in some countries. Nevertheless, they will strongly influence the profitability of energy systems and should thus be included in an economic assessment. In this work, the focus lies on the development in Germany and three scenarios are deduced.
The first scenario reflects an old policies scenario. Here, no carbon pricing is introduced which is referred to as the no costs scenario (NC scenario). In addition, a low costs scenario (LC scenario) is introduced. As the German government discusses the option to introduce a lower boundary of 35 €/t for carbon pricing starting in 2027. In the LC scenario, this is assumed to stay constant until 2030. In contrast to that, a third scenario is evaluated in which the future trend for pricing carbon from 2021 until 2025 is extrapolated resulting in a price of 66 €/t in 2030. We refer to this scenario as high costs scenario (HC scenario).

3.2.2. Future CO_2 factor

When evaluating the costs for carbon, it is necessary to predict the mass of CO_2 emissions caused by the respective energy system. In this context, CO_2 factors play an important role as they allow to estimate the CO_2 emissions per kWh of an energy source.
Since it depends on the chemical properties of an energy source, its CO_2 factor does not underlie time-dependent changes in most cases. This applies, for example, to natural gas (approx. 202 g/kWh) and heating oil (approx. 266 g/kWh).
Due to the Energiewende the composition of the so called electricity-mix in Germany and likewise its CO_2 factor are subject to steady changes. The past development and a prediction of this CO_2 factor is shown in figure 3. As the share of RE in the electricity mix has the highest impact on the CO_2 factor, the prediction is calculated with a linear function of this share. This function is based on past data points of the CO_2 factor and RE share in Germany. The future development of the RE share itself is also a linear function with the goals of the German government being the interpolation points. Obviously, the CO_2 factor will decrease in the next years due to an increasing RE share. Additionally, it is shown that by 2042 the CO_2 factor of electricity will be lower than the factor of gas.

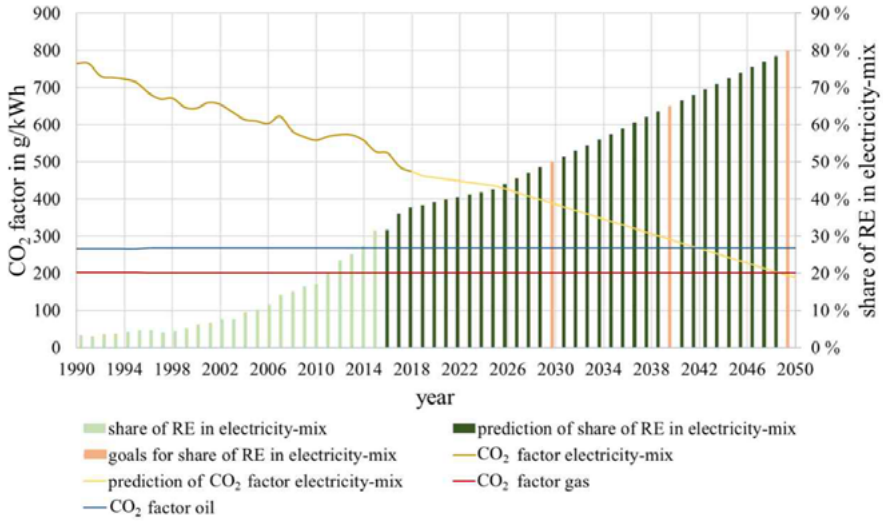

Fig. 3. Development of the CO_2 factor of the average German electricity mix in recent years and in the future. The CO_2 factors of gas and oil are given as benchmarks.

The presented methodology enables the simulation-based assessment of the two developed supply scenarios. As a result, we obtain the operating costs of the system which depend on the energy prices and the CO_2 factor respectively.

3.2.3. Key performance indicators

Based on the deduced energy prices and CO_2 factors the two scenarios are compared. In order to evaluate the systems from an ecological point of view on the one hand, the annual CO_2 emissions caused by the cooling and heating system are calculated. On the other hand, the system´s annuity is used to compare the profitability of the two scenarios. The annuity calculation bases on the German guideline VDI 2067 [26]. According to VDI 2067 the annuity consists of 3 cost types: the capital- (cap), demand- (dem), and operation-related costs (op). The capital-related costs are based on a market analysis on component investment costs. The demand-related costs derive from the simulation results and the electricity, gas as well as carbon prices of the respective year (s. chapter 3.2.1. and 3.2.2.). The operation-related costs are calculated as a fixed percentage of the capital-related costs which depend on the component type [26]. The annuity-based capital-related costs depend on the component service life. The components considered are the HP, the chiller, the CGB and the electrical heater.

Results and discussion

The resulting thermal demands of the FUBIC building are shown in figure 4. The heating power is mostly required in the cold season (September to April). At the start of the simulation, a considerable heat demand is detected as a result of the initialization process but not taken into account for the demand analysis.
Regarding the cooling demand, a base load of around 80 kW covered by the additional cooling can be identified throughout the entire period (additional cooling). This is caused by the cooling demand of the servers. The dynamic cooling demand, however, is primarily required for cooling and dehumidification of the outdoor air in the warm season (May to August).

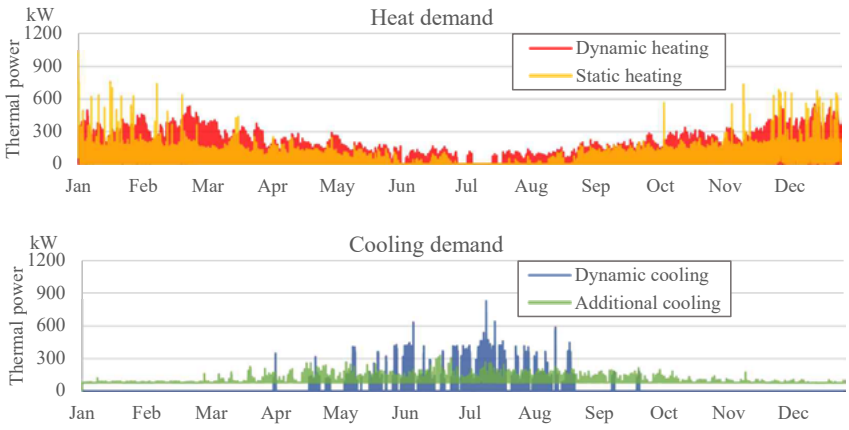

Fig. 4. Simulated heat (above) and cooling (below) demands of the FUBIC building using a TRY with a cold winter.

The presented thermal demands are the basis for the choice of a supply system. The simultaneous occurrence of heating and cooling demand e.g. impedes the use of a reversible HP. This is why a chiller has to be implemented in order to meet the cooling demand throughout the whole year. Nevertheless, a major advantage of HPs over CGBs is that while generating heat at a high temperature level at condenser site they extract heat at evaporator site at a lower temperature level at the same time. Usually, the extracted heat is taken from the ambient air or ground. However, as FUBIC´s heating and cooling demand occur simultaneously, the extracted heat can be used to partially cover the cooling demand. In this use case, the interaction is realized by a hydraulic connection via the ice storage. Here, the HP´s evaporator as well as the chiller´s evaporator are hydraulically connected via the ice storage. Hence, both the HP and the chiller can cover the cooling demand and synergy effects can be realized.

Based on the given energy demand structure, the two presented supply scenarios are assessed. Figure 5 depicts the simulation results. We compare the annual CO_2 emissions as well as the resulting negative annuity of the conventional (C) and the HP-based all-electric scenario (AE) in 2018 and in 2030. The annuity is negative in all scenarios as only costs are considered in this study. The biggest share in total costs are the demand-related costs. They make up 82 to 90 % of the annuity depending on the regarded scenario.
In 2018, the annuity of the conventional scenario is 35 % lower compared to the all-electric scenario. This effect is explained by lower gas prices per kWh in comparison to electricity prices in Germany as well as lower capital-related costs. CBGs´ capital-related costs are 50 % lower than those of HPs.
From an ecological point of view, the conventional scenario leads to an increase in CO_2 emissions of 2 % in 2018. However, this does not have any effect on the operating costs as carbon is not priced yet in Germany. Consequently, given the present boundary conditions, the all-electric system is not more profitable than the conventional scenario. The savings in CO_2 emissions are negligible as the current electricity mix in Germany is still mainly based on conventional energy sources.

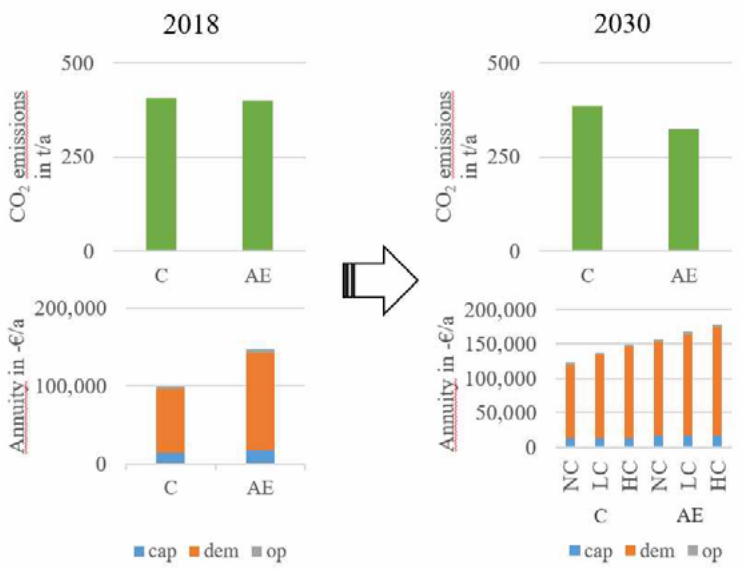

Fig. 5. Comparison of CO_2 emissions and annuity of the conventional and HP-based all-electric scenario for 2018 (left) and 2030 (right). In 2030, two scenarios for future CO_2 pricing are considered (NC = no costs; LC = low costs; HC = high costs). The system annuity is divided into the annual capital- (cap), demand- (dem) and operating-related (op) costs.

In 2030 however, the three introduced carbon pricing scenarios (NC, LC, HC) are taken into consideration which have an effect on the demand-related costs. As the share of REs in the German electricity mix increases, overall CO_2 emissions for both scenarios decrease. So even if the electricity consumption remains the same in 2030, overall emissions will be lower as the CO_2 factor of electricity decreases (s. figure 3). This effect is not applicable for the CO_2 emissions caused by the CGB. As explained in chapter 3.2.2., the CO_2 factor of gas depends on the chemical structure only and thus will remain constant in the future. As a result, the difference in CO_2 emissions in 2030 between the regarded scenarios increases to 18 %. Obviously, all-electric systems lead to higher CO_2 emission savings in the future. The reduction of CO_2 emissions simultaneously leads to decreased operating costs in 2030 due to carbon pricing.

Despite this effect, the system annuity of the conventional system is lower compared to the HP-based all-electric system in all of the regarded carbon pricing scenarios. This can be explained by the low percentage of carbon costs in the total demand-related costs. In the conventional scenario, costs for CO_2 emissions make up 11 and 19 % in the LC and HC scenario respectively. In the HP-based all-electric scenario, however, carbon costs only account for 8 and 14 % (LC and HC scenario respectively). Obviously, even though the carbon costs double in the HC scenario compared to the LC scenario, they do not influence the overall trend significantly.
For the given comparison, we calculate a break-even price for CO_2 of 559 €/t which results in equal annuity in the conventional and the all-electric scenario. Based on the researched forecasts for carbon pricing in 2030, we assume this to be unlikely.

Based on the results, regarding external boundary conditions the development of electricity and gas prices will more importantly influence the profitability of energy systems. In our use case, costs for gas and electricity make up 81 to 92 % of the demand-related costs. Even though the energy price´s influence decreases in the future as CO_2 prices will presumably be introduced, they still account for the biggest percentage in annuity. Nevertheless, in the conventional scenario, the demand-related costs increase by 80 % in the LC and by 99 % in the HC scenario. In the LC (HC) scenario, this increase is caused to an extent of 61 % (66 %) by the introduction of carbon pricing and to 39 % (34 %) by the rising gas prices.
Given the two regarded scenarios, the break-even gas price is 7.2 ct/kWh and the break-even electricity price is 11.1 ct/kWh.
Consequently, the HP-based all-electric scenario can be profitable only considering external boundary conditions in the future if either the gas price increases or the electricity price decreases in the large customer

segment. Another key factor is the system efficiency. HPs´ COP strongly depends on external influences such as the ambient temperature. In our case, a test reference year with a cold winter was chosen which decreases HP´s COP significantly. Advanced energy management systems can increase system efficiency by shifting HP´s operation e.g. to times of higher ambient temperatures. In addition, they enable the efficient coordination of heating rod and HP as we focus on a bivalent system.

4. Conclusions and Outlook

In this study, the assessment of a common conventional CGB-based and a HP-based all-electric energy supply scenario reveals that HP-based energy systems are not necessarily more profitable in the future. It becomes obvious that considering the regarded three cost types, the demand-related costs (CO_2 emissions costs and costs for electricity/gas) make up the highest percentage.
Irrespective of the carbon pricing scenario, the conventional scenario´s annuity is lower despite its higher emissions. The break-even price for CO_2 is 559 €/t which is assumed to be unrealistic. Hence, carbon pricing should be taken into consideration as it influences economic evaluation but it is not the main cost driver. In addition, we calculate the break-even gas price which is 7.2 ct/kWh and the break-even electricity price which is 11.1 ct/kWh for the large customer segment. Obviously, HP-based all-electric supply systems become more profitable once gas prices increase or electricity prices decrease.

Apart from that, we prove that conventional supply systems are not necessarily more suitable for non-residential buildings with complex energy demand structures. In the presented use case, heating and cooling demand occur simultaneously and are highly fluctuating. In this context, a HP-based energy system enables the exploitation of synergy effects between the heating and cooling systems. As HPs supply heat on condenser site while extracting heat on evaporator site, heating and cooling demand can be covered simultaneously. Nonetheless, a chiller and an electrical heater should be integrated to ensure secure energy supply throughout the whole year. This synergy effect cannot be accomplished by a conventional technology such as the CGB and needs an advanced energy management system for efficient operation.

All in all, profitability of HP-based all-electric systems mainly depends on the demand-related costs. Besides from external boundary conditions such as the given prices for electricity and gas, these costs can be decreased by high system efficiency. Intelligent operating strategies and an advanced energy management system support the profitability of HP-based all-electric systems. For the use case presented in this study, the focus should lie on the complex interaction of the heating and cooling system as they are coupled via an ice storage.

Acknowledgements

We gratefully acknowledge the financial support by Federal Ministry for Economic Affairs and Energy (BMWi), promotional reference 03ET1619B.

References

[1] Statistisches Bundesamt (Destatis). Bauen und Wohnen: Baugenehmigungen/Baufertigstellungen von Wohn- und Nichtwohngebäuden (Neubau) nach Art der Beheizung und Art der verwendeten Heizenergie 2018, 2019. Available at: https://www.destatis.de/DE/Themen/Branchen-Unternehmen/Bauen/Publikationen/Downloads-Bautaetigkeit/baugenehmigungen-heizenergie-pdf-5311001.pdf?__blob=publicationFile – [accessed 15.11.2019].
[2] Agentur für Erneuerbare Energien, 2019. Available at: https://unendlich-viel-energie.de/mediathek/grafiken/endenergieverbrauch-2017-nach-strom-waerme-und-verkehr – [accessed 15.11.2019].
[3] V1.5 Energiedaten; Geschäftsstelle der Arbeitsgruppe Erneuerbare Energien-Statistik (AGEE-Stat), Erneuerbare Energien in Zahlen, 2019. Available at: https://www.umweltbundesamt.de/themen/klima-energie/erneuerbare-energien/erneuerbare-energien-in-zahlen#textpart-1 – [accessed 15.11.2019].
[4] Lauf, Dr. T., Memmler, M., Schneider, S., 2019. Emissionsbilanz erneuerbarer Energieträger. Available at: https://www.umweltbundesamt.de/daten/energie/energieverbrauch-nach-energietraegern-sektoren – [accessed 15.11.2019].
[5] Bürger, V., Hesse, Dr. T., Quack, D. , Umweltbundesamt. Klimaneutraler Gebäudebestand 2050, 2016. Available at: https://www.umweltbundesamt.de/sites/default/files/medien/378/publikationen/climate_change_06_2016_klimaneutraler_gebaeudebestand_2050.pdf – [accessed 15.11.2019].

[6] Bundesministerium für Umwelt, Naturschutz, Bau und Reaktorsicherheit, Klimaschutzplan 2050. Klimaschutzpolitische Grundsätze und Ziele der Bundesregierung, 2016. Available at: https://www.bmu.de/fileadmin/Daten_BMU/Download_PDF/Klimaschutz/klimaschutzplan_2050_bf.pdf – [accessed 15.11.2019].
[7] Gerhardt, N., Fraunhofer-Institut für Windenergie und Energiesystemtechnik Geschäftsmodell Energiewende: Eine Antwort auf das "Die-Kosten-der-Energiewende"-Argument, Kassel, 2014.
[8] dena Deutsche Energie-Agentur, Statistiken und Analysen zur Enegieeffizienz im Gebäudebestand. Available at: https://www.dena.de/fileadmin/user_upload/8162_dena-Gebaeudereport.pdf – [accessed 15.11.2019].
[9] Ranft, F., Institut für Technik und Ökologie, Neubau eines energetisch optimierten Bürogebäudes Bob – balanced office building. Endbericht., 2007. Available at: www.enob.info/fileadmin/media/Publikationen/EnBau/Projektberichte/ 19_MonitoringAB_1_p2_BOB_k.pdf. – [accessed 15.11.2019].
[10] BWP-Bundesverband Wärmepumpe e.V., BWP-Branchenstudie 2015: Szenarien und politische Handlungsempfehlungen, 2015. Available at: https://www.waermepumpe.de/fileadmin/userupload/waermepumpe/07_Publikationen/2016-04-08_Branchenprognose_2015_web.pdf. – [accessed 15.11.2019].
[11] Jochum, P., Lempik, J., Böttcher, S., Stelter, D., Krenz, T., Mellwig, P., Pehnt, M., von Oehsen, A., Blömer, S., Hertle, H., Beuth Hochschule für Technik Berlin, ifeu- Institut für Energie- und Umweltforschung Heidelberg GmbH, Ableitung eines Korridors für den Ausbau der erneuerbaren Wärme im Gebäudebereich, 2017.
[12] Nitsch et al., Deutsches Zentrum für Luft- und Raumfahrt (DLR), Institut für Technische Thermodynamik, Fraunhofer Institut für Windenergie und Energiesystemtechnik (IWES), Langfristszenarien und Strategien für den Ausbau der erneuerbaren Energien in Deutschland bei Berücksichtigung der Entwicklung in Europa und global, 2012. Available at: https://www.dlr.de/dlr/Portaldata/1/Resources/bilder/portal/portal_2012_1/leitstudie2011_bf.pdf – [accessed 15.11.2019].
[13] Huchtemann K., Müller D., 2012, Evaluation of a field test with retrofit heat pumps. Building and Environment; p.100–106.
[14] Bundesministeriums für Umwelt, Naturschutz und nukleare Sicherheit, Klimaschutz in Zahlen: CO_2-Bepreisung. Available at: https://www.bmu.de/fileadmin/Daten_BMU/Download_PDF/Klimaschutz/pcd_co2_bepreisung_bf.pdf – [accessed 15.11.2019].
[15] Klimakabinett, Eckpunkte für das Klimaschutzprogramm 2030, 20.09.2018. Available at: https://www.bundesregierung.de/resource/blob/975202/1673502/768b67ba939c098c994b71c0b7d6e636/2018-09-20-klimaschutzprogramm-data.pdf?download=1 – [accessed 15.11.2019].
[16] Müller D., Lauster M., Constantin A., Fuchs M., Remmen P., AIXLIB–An open-source Modelica Library within the IEA-EBC Annex60 framework. In: Grunewald J., Felsmann C., editors. Proceedings of the CESBP Central European Symposium on Building Physics and BauSIM 2016; 2016 Sep 14-16; Dresden, Germany. Fraunhofer IRB Verlag:3-9.
[17] Swiss Society of Engineers and Architects – Raumnutzungsdaten für die Energie- und Gebäudetechnik (SIA 2024), Zürich, Switzerland, 2015.
[18] The Association of German Engineers, Guidline 6007, Part 1: Calculation of transient thermal response of rooms and buildings - Modelling of rooms, Beuth Verlag GmbH, Berlin, Germany, 2012.
[19] Remmen, P., Lauster M., Mans M., Osterhage T., and Müller D. (2016). Citygml import and export for dynamic building performance simulation in modelica. In Proceedings of the 3rd IBPSA-England Conference BSO 2016.
[20] Deutsches Institut für Normung e.V., DIN V 18599 – Energy efficiency of buildings – Calculation of the net, final and primary energy demand for heating, cooling, ventilation, domestic hot water and lighting. Beuth Verlag GmbH, Berlin, Germany, 2018.
[21] Siemens AG, Regeln und Steuern von Lüftungs-/Klimaanlagen, 2018. Availablte at: https://www.downloads.siemens.com/download-center/Download.aspx?pos=download&fct=getasset&id1=A6V10327348 – [accessed 15.11.2019].
[22] Deutscher Wetterdienst DWD, Ortsgenaue Testreferenzjahre von Deutschland für mittlere, extreme und zukünftige Witterungsverhältnisse. Offenbach, 2017.
[23] Deutsches Institut für Normung e.V., DIN 4701-10, Energy efficiency of heating and ventilation systems in buildings – Part 10: Heating, domestic hot water, ventilation, Beuth Verlag GmbH, Berlin, Germany, 2003.
[24] Zottl A., Nordman R., Miara M., Benchmarking method of seasonal performance: D4.4 Benchmarking method of seasonal performance under consideration of boundary conditions. Available at: http://sepemo.ehpa.org/uploads/media/D4_4_reporting_Benchmarking_method_of_seasonal_performance.pdf – [accessed 15.11.2019].
[25] ewi Energy Research & Scenarios gGmbH , Energiemarkt 2030 und 2050 –Der Beitrag von Gas-und Wärmeinfrastruktur zu einer effizienten CO2-Minderung, 2017. Available at: https://www.ewi.research-scenarios.de/cms/wp-content/uploads/2017/11/ewi_ERS_Energiemarkt_2030_2050.pdf – [accessed 15.11.2019].
[26] VDI Verein Deutscher Ingenieure e.V., VDI 2067: Economic efficiency of building installations. Berlin: Beuth Verlag GmbH; 2012.

13th IEA Heat Pump Conference
April 26-29, 2021 Jeju, Korea

Long-term evaluation of an office building with large-scale heat pump and aquifer system in southern Sweden

Tommy Walfridson[a], Martin Larsson[b], Jessica Benson[c], Oskar Räftegård[d], Ola Gustafsson[b], Caroline Haglund Stignor[b], Lovisa Axelsson[c], Pia Tiljander[b]

[a] Energy and Circular economy, RISE Research Institutes of Sweden, Stockholm , Sweden
[b]Energy and Circular economy, RISE Research Institutes of Sweden, Borås, Sweden
[c]Energy and Circular economy, RISE Research Institutes of Sweden, Göteborg, Sweden
[d]Energy and Circular economy, RISE Research Institutes of Sweden, Karlstad, Sweden

Abstract

IEA Annex 52 is the first long-term evaluation of large-scale heat pump systems. The Annex aims to survey and create a library of quality long-term measurements of GSHP system performance for commercial, institutional and multi-family buildings. The IEA Annex 52 also aims to provide a set of benchmarks for comparisons of such GSHP systems around the world.

The GSHP system in this report consists of two serial coupled heat pumps connected to a four-well aquifer and produces both heating and cooling. Total heating capacity is 0.3 MW. Due to a complex system with poor control system the Seasonal Performance Factor, SPF_{H4} is as low as 2.5 for the first year. Several control errors have been identified, including a potential short circuit of the serial DHW heat pump, erroneous operation of it for heating purpose and probable unnecessarily high condensation temperatures of the main heat pump.

The cooling system has high Seasonal Performance Factor, SPF_{C4} is 5.7 the first year. The system mainly uses free cooling, but performance decreases significantly at low load, possibly due to poor pump control. All system boundaries used are the IEA Annex 52 proposal

Selection and/or peer-review under responsibility of the organizers of the 13th IEA Heat Pump Conference 2020.

Keywords: System performance; System boundaries; Large-scale heat pump system; Annex 52 long-term evaluation; Performance Factor, Coefficeint of Performance; Office; GSHP; Sweden;

1. Introduction

1.1 Background

Measured long-term performance data for ground source heat pump systems serving commercial, institutional and multi-family buildings are rarely reported in the literature [1].

IEA HPT Annex 52 [2] is focused on long term performance measurement of GSHP systems serving commercial, institutional and multi-family buildings. Performance varies between different plants, and there is a need of more knowledge of the underlying causes. An important part of Annex 52 is to develop a methodology for measurement strategies and common system boundaries for larger heat pump systems. To achieve this 40 GSHP monitoring case are studied, covering a range of applications, located in seven countries.

It is important to make analyses based on a large amount of data and to identify key performance indicators when comparing different heat pumps.

More information with focus on factors that influence the performance is needed, identifying causes of low performance and unnecessary errors that can be avoided in the future. One example that causes low

performance of a GSHP system is for example dimensioning issues and suboptimal control systems. Reasons of low performance needs to become visible, in order to get knowledge and understanding.

The over-all performance of a GSHP system is affected by the performance of the source side ground circuit, as well as the heat pump unit performance and the load side circuit performance, including supplementary heating and cooling. The varying design and complexity of GSHP systems poses challenges in comparable performance factors.

Detailed long-term analyses of large GSHP systems for commercial, institutional and multifamily buildings are rare. This article describes one of the 40 GSHP monitoring case studies and focuses on evaluating an aquifer heat pump system. The system design is described, and Seasonal Performance Factors (SPF) are analyzed from 2 years of measurement data.

1.1.1 System boundaries

The IEA Annex 52 project has identified the need of and proposed system boundaries for large-scale GSHP system [3] based on the 2012 SEPEMO work [4]. The system boundaries are shown in Figure 1 below. The system boundaries used in this report are 0, 1 and 4. System boundary 0 is the aquifer system, including pumps and are discussed in chapter 3.1, system 1 is inside the heat pump cabinet and is estimated in chapter 3.2. The project has good measurements for system boundary 4, this is examined in chapter 3.3

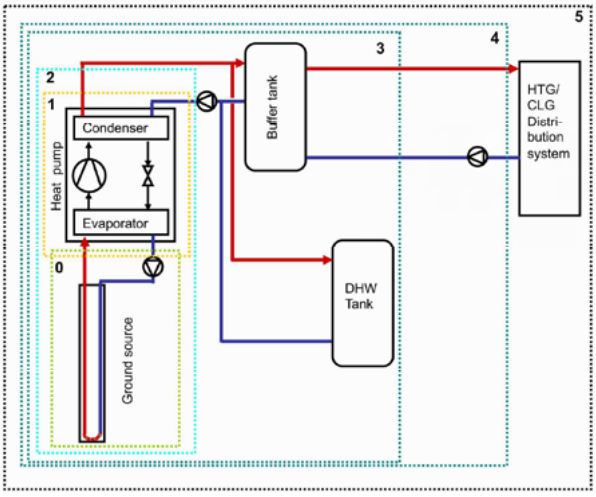

Figure 1 System boundaries according to the IEA Annex 52 project proposal (preliminary)

2 Methodology

One aim of the project is to aid the Annex 52 project in finding relevant system boundaries and test them. Another is to evaluate the performance of the GSHP system and find Performance Factors on the different system boundaries, whenever possible to calculate. This project has historic data from 2012-2014, data that previously was analyzed by RISE in an earlier, different project. No newer measurements have been used, but few changes have been made to the system until today, meaning the data is still valid for the system. The data set consist on electrical energy metering on each heat pump and summed on all circulation pumps and energy metering on aquifer, cooling, heating, subcooler heat and Domestic Hot Water, DHW, all on hourly basis. Temperatures were only measured at the four wells of the aquifer; no additional temperature data is available. Outdoor temperatures were taken from the SMHI [5] weather station at the nearby airport, corrected due to the site's much closer distance to a large lake and the elevation difference (140 m). The temperature was corrected +0,8°C, which was the annual temperature difference between the now closed city weather site and the still operating airport weather site, when comparing historic data. This approach is not perfect, as the variation is great and the temperature difference is slightly higher in the winter, but no better correction was found.

To understand the project a site visit was performed in October 2019.

2.1 Object

The heat pump and aquifer system serving an office building is located in southern Sweden, with undisturbed ground temperature of about 6 °C. One advantage offered by aquifers is the seasonal storage and another that different temperatures effectively could be stored separately, by using cold and warm wells. Essential for good performance is to optimise temperature-levels, for optimal use of the advantageous temperatures of aquifers. The system is described in Figure 2.

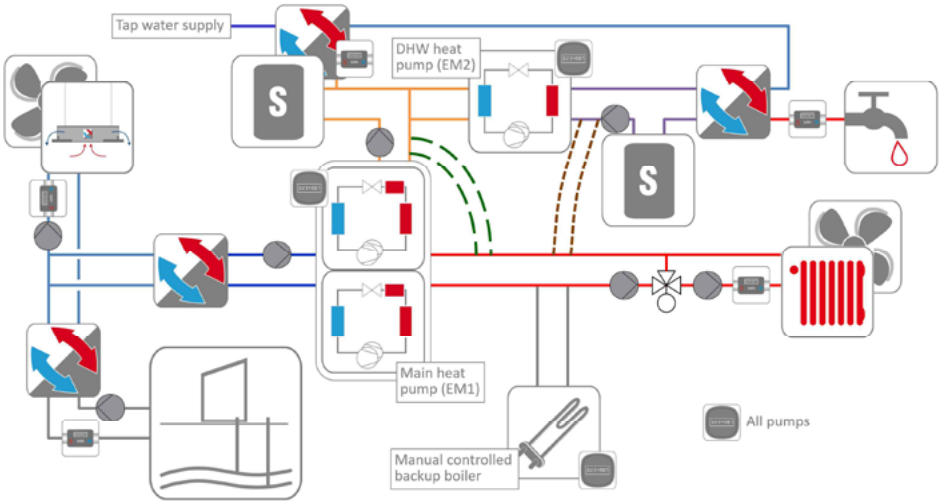

Figure 2 The heat pump and aquifer system. The Main heat pump (EM1) is using the aquifer as its heat source, while the DHW heat pump (EM2) is using the subcooler of the Main heat pump as its heat source. Dashed green and brown lines show possible heat flows, flows that are not intended according to the documentation, but are fully possible. All functionality is not described and especially the dashed lines are symbolically drawn. Pictograms by TU Braunschweig IGS, used with permission within the course of IEA HPT Annex 52

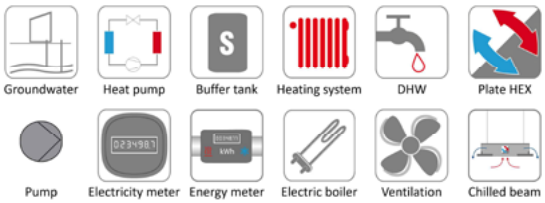

Figure 3 Explanation of pictograms used in Figure 2. Note that the heat pumps used are all dual compressor heat pumps and the main heat pump has subcooler heat exchangers. Pictograms by TU Braunschweig IGS, used with permission within the course of IEA HPT Annex 52

The main heat pump (EM1) has a heating capacity of about 300 kW and has four compressors in two refrigerant circuits, see Figure 2. The main heat pump (EM1) uses the aquifer as the heat source, while the Domestic Hot Water (DHW) heat pump uses the subcooler of the main heat pump as the heat source. The condenser of the main heat pump (EM1) heats the building, but with a change of two valves, the DHW heat pump can also heat the building. At times with to low heating capacity of the subcooler, the condensor has the possibility to heat the DHW as well, see dashed curved lines of Figure 2. The cooling system in the building is, via two heat exchangers, connected to the aquifer and the evaporator of the main heat pump. According to design documentation the main heat pump is used for heating, with temperature aid from the DHW heat pump during winter conditions with need of high heating system temperatures. The subcooler has a setpoint of 20°C, giving the DHW heat pump the possibility of high Coefficient of Performance (COP) when producing DHW.

The setpoints of the heating system is 35°C at an ambient temperature of 0°C and 50°C at dimensioning ambient winter temperature (-18°C), meaning a relatively low temperature system.

The strategy of the control system is to keep the condensing temperature of the Main heat pump (EM1) as low as possible. The main heat pump is used for heating only, the control system can not start it for cooling purpose, regardless of cooling demand. The cooling capacity is regulated by the flow from the aquifer, it has no dependency control wise to the heat pump. There is a need of cooling all year round. The cold wells of the aquifer are used at ambient temperatures above 12 °C, while the warm wells are used below 10 °C. There is no other hysteresis in changing the well of the aquifer, meaning the wells will be changed many days of the year. According to the site visit the wells are now (2019) changed manually instead.

2.2 Method

2.2.1 Calculation method

An estimated Performance Factor for heating on system boundary 1, PF_{H1}, for the main heat pump was calculated using the following formula:

$$PF_{H1} \approx \frac{Q_{Heating\ system} + Q_{Subcooler\ DHW} + Q_{DHW} - P_{EM2}}{P_{EM1}} \quad (1)$$

The only measurement done on the system boundary 1 for the main heat pump (EM1) is its own power consumption, P_{EM1}. The heat from the subcooler to preheat the DHW, $Q_{Subcooler\ DHW}$ and the heat to the heating system, $Q_{Heating\ system}$, are measured on system boundary 4. All energy supplied by the system originates from the main heat pump, the DHW heat pump is only increasing the temperatures. This means that the power consumption of the DHW heat pump, P_{EM2}, should be subtracted from the total heat supplied to calculate the performance factor of the main heat pump (EM1), PF_{H1}. As losses in the system are not stringently taken into account this can only be considered an estimate.

To be able to calculate Performance Factors on system boundary 4 the power consumption of the circulation pumps and the heat pump compressors must be allocated to the heating and the cooling side. This is done based on the heat and cooling produced for each hour of the year, according to the consensus in the Annex 52 project group. Power consumption allocated for cooling is calculated according to:

$$P_{Cooling\ ,allocated} = \left[\frac{Q_{Cooling}}{Q_{Cooling} + Q_{Heating\ system}}\right] \cdot \left(P_{EM1} + P_{pump\ ps}\right) \quad (2)$$

While power consumption allocated for heating is calculated according to:

$$P_{Heating\ ,allocated} = \left[\frac{Q_{Heating\ system}}{Q_{Cooling} + Q_{heating}}\right] \cdot \left(P_{EM1} + P_{pump\ ps}\right) + P_{EM2} \quad (3)$$

All circulation pumps are measured combined with one electrical energy meter; thus, the dedicated cooling or heating system pumps could not be allocated directly to their side of the system. All circulation pump power consumption is thus allocated according to the formulas, as this was the best possible method. The compressor power consumption of the EM2 is only used to produce DHW and does not cool the aquifer, all that power consumption is allocated to the heating side.

The calculation of the Performance Factor for heating on system boundary 4, PF_{H4}, is calculated with the following formula:

$$PF_{H4} = \frac{Q_{Heating\ system} + Q_{Subcooler\ DHW} + Q_{DHW}}{P_{Heating\ ,allocated}} \quad (4)$$

The calculation of the Performance Factor for cooling on system boundary 4, PF_{C4}, is calculated with the following formula:

$$PF_{C4} = \frac{Q_{Cooling}}{P_{Cooling\ ,allocated}} \quad (5)$$

In this paper performance factor SPF and DPF are used, were SPF is calculated over one year and DPF is calculated over 24 hours.

3 Results (Discussion)

The office building has a heating and cooling load according to Figure 4 below, the diagram has 24h average values due to low resolution of energy data.

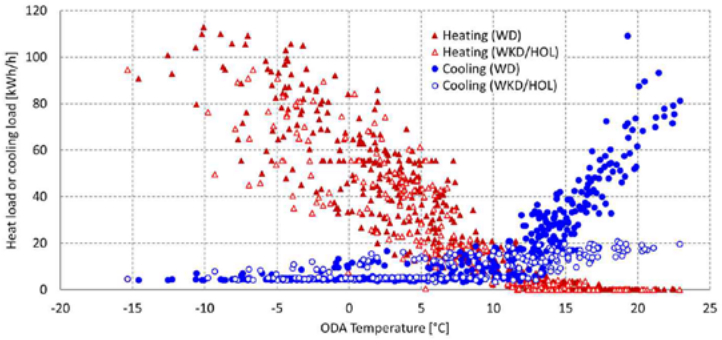

Figure 4 Heat and cooling load as a function of outdoor temperatures, average over 24h

As seen in Figure 4 the cooling load is highly dependent on the activities of the employees, during weekends and holidays the cooling load is a fraction of the workdays. The same is not seen in heating, but the variations at the same outdoor temperatures is very large. This could be due to the weather (sun/cloud) as the building has very few shadowing buildings surrounding it, but no data could verify this.

A thermal balance of the entire system was done, showing good results, see Figure 5. The negative side is sources of heat: The warm well of the aquifer, the compressors of the two heat pumps and the pumps in the system. The positive side is the sink of heat: The cold wells of the aquifer, the heating system and the Domestic Hot Water (DHW)

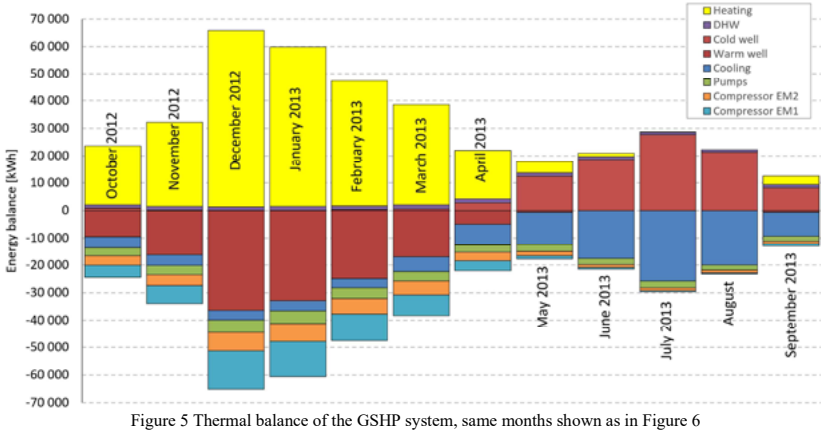

Figure 5 Thermal balance of the GSHP system, same months shown as in Figure 6

Total pump power consumption is high at low load conditions, especially compared to compressor power consumption.

3.1 IEA Annex 52 system boundary 0

The energy extracted and injected into the aquifer was measured, but as seen Figure 6, the resolution is low (100 kWh per pulse). As the pump of the aquifer were not measured separately no Performance Factor could be derived. In order to express the energy in kWh/h a 24-hour average value was calculated.

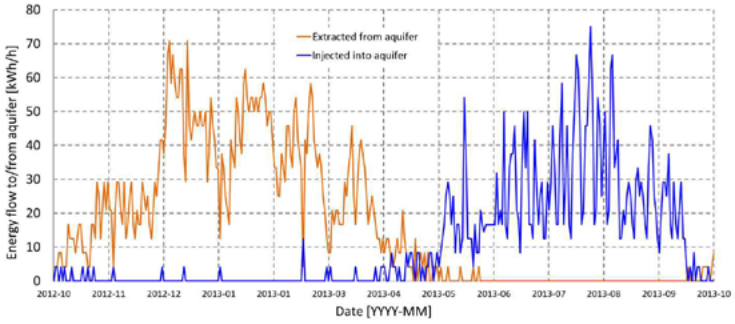

Figure 6 Heat extracted from and injected into the aquifer during one full year, mainly the first year in the time series, 24h average.

As seen in the diagram the pumps are at several occasions reversed, especially in April, May, September and October. The16th of February, a cold day, the pumps reverse, and the cold well was used, clearly seen in Figure 6. The control system didn't handle the aquifer optimal, as mention in chapter 2.1 the flow direction of the aquifer was change just according to ambient temperature, meaning the flow direction changes often in the spring and autumn. According to a site visit (2019) this was now handled manually instead.

3.2 IEA Annex 52 system Boundary 1

3.2.1 Heating

The measured data of the office building is not enough to calculate the performance on individual heat pump level but it could be estimated by subtracting the power consumption of the DHW heat pump (EM2) from the total heat produced, see equation 1 in chapter 2.2.1. The only function of the DHW heat pump is to increase the temperature from the main heat pump (EM1), EM2 has the main heat pump (EM1) as its only heat source, see Figure 2. The heating Seasonal Performance Factor on system boundary 1, SPF_{H1} is estimated to 4.2 the first year and 3.7 the second year, when the DHW heat pump has a better control strategy. See chapter 3.4 for further details and discussion.

3.3 IEA Annex 52 System Boundary 4

On system boundary 4, see to Figure 1 for definition, meaning the entire heat pump installation, excluding the heating, cooling and ventilation system of the building itself, all necessary data has been measured over the period September 2012 to August 2014. The allocation of pump and compressor power consumption is seen in equations 2 and 3, while the Performance Factors are calculated according to equations 4 and 5, all in chapter 2.2.1

3.3.1 Heating

The following diagram over Daily Performance Factor, DPF, see Figure 7, has been developed to fully understand the performance of a heat pump system at a glance. It directly shows that the heat pump system, with four compressors in the main heat pump (EM1) and a total heating capacity of 300 kW, is oversized and only uses one compressor in on/off mode most of the year. The maximum capacity used is 110 kW or 37 % of installed capacity, despite both winters during the period having low temperatures. It also directly shows that the heat pump system has almost the same performance factor regardless of heat output and that it at very low output mainly collapses in performance.

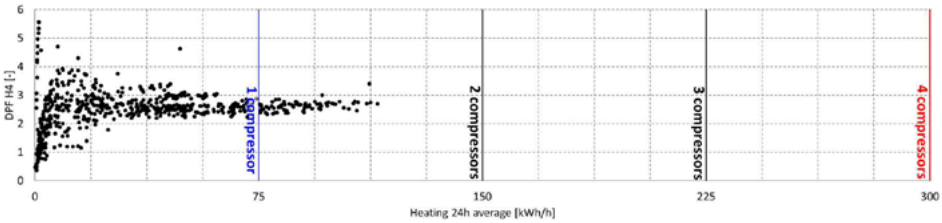

Figure 7 Overview of heat pump system performance factor H4 as a function of heat provided to the office building, blue line shows lowest capacity without ON/OFF operation, red line maximum heating capacity at highest heating system temperatures (winter)

The heat pump system has been compared to a state-of-the-art heat pump system produced by a major Swedish manufacturer in order to show the expected performance for a well-designed system, see Figure 8 below.

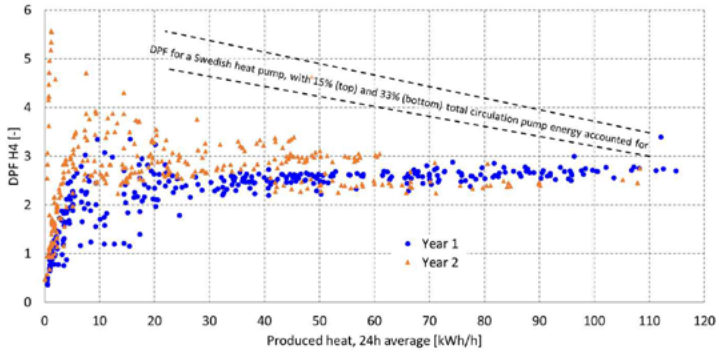

Figure 8 The heat pump system heating Daily Performance Factor, DPF_{H4}, compared a state-of-the-art heat pump system

The second year the control system is changed September 16th, 2013, it is noted as a significant decrease of power consumption of the DHW heat pump (EM2), but exact implication of the change is not known. This clearly increases performance in the medium output region, but the change is reversed between January 15th 2014 and March 4th 2014, giving poor performance in the high output region again. The change is likely done for the system to be able to deliver high enough temperature to the heating system, but that has not been possible to verify, as temperature data is not available.

The heat pump system is within the range of the total pump energy seen in Figure 8 above (dashed lines), 15-33 % of total compressor power consumption, above 40 kWh/h average produced heat. Below 40 kWh/h pump energy increases dramatically and is 90% at lowest heating load. This indicates a systematic error in the control of circulation pumps, which could not be explained by the nature of the aquifer system.

It is difficult to understand that the DPF_{H4} is below one (1) at low capacity, worse than resistive heating, but the control of the aquifer pumps is likely a major cause. The exaggerated pump power then gives very little heat to the brine system, as little is being needed, the losses in the water-cooled pumps basically heats the aquifer instead.

The Seasonal Performance Factor, SPF_{H4}, is calculated to 2.5 for the first year and due to the change in the control system the SPF_{H4} increased to 2.7 the second year. For a well-designed heat pump system, the SPF_{H4} is estimated to be able to reach 4 in the office building, around 50 % higher than the system used.

3.3.2 Cooling

The heat pump system is used to cool the building, it has a fairly constant equipment cooling load of 4-6 kWh/h clearly seen during heating season, but the main cooling load is during the short Swedish summer in June, July and August.

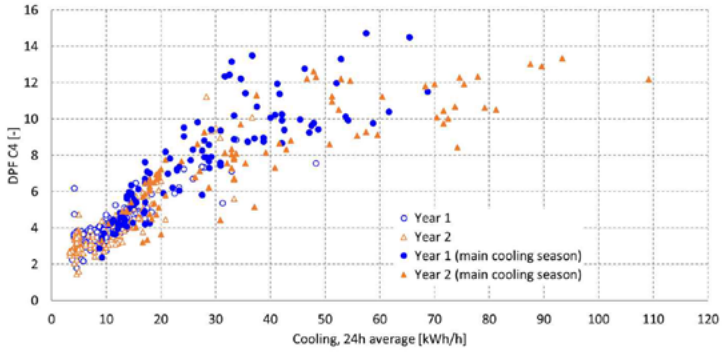

Figure 9 The heat pump system cooling Daily Performance Factor, DPF_{C4}

As seen in Figure 9 the Daily Performance Factor, DPF_{C4}, is high or very high during most of the year, but at low load the performance is in parity with conventional chiller performance. It is clear from the data that the cooling is mainly produced directly from the aquifer, by means of free cooling, else this high performance would be impossible. The low performance at low load is likely due to poor control of the aquifer pumps, note that the performance is low at low load even at the main cooling season, with very low heating demand, see filled markers in Figure 9. The performance is thus not mainly an effect of the method used for allocating the pump electricity. Note that the power consumption of the DHW heat pump (EM2) is not affecting the cooling Performance Factor, it is accounted on the heating side only, see chapter 2.2.1.

A well performing aquifer system, with good pump management at lower load, could perform at the top performance seen in Figure 9 most or all of the cooling season.

The Seasonal Performance Factor, SPF_{C4}, is calculated to 5.7 for the first year and slightly higher 5.8 the second year

3.4 The serial DHW heat pump (EM2)

The DHW heat pump (EM2) has the subcooler of the main heat pump (EM1) as its main heat source, it can not use the aquifer directly as a heat source. The DHW heat pump (EM2) is designed to mainly produce Domestic Hot Water, DHW, but can aid the main heat pump (EM1), only producing heat, to keep high enough temperature in the heating system. This means that the DHW heat pump (EM2), at DHW production, should use significantly less power than the main heat pump (EM1), else the thermal balance is not fulfilled. The reason being the subcooler of the main heat pump produce a fraction of the total condenser heat and varying depending on condensing temperature. The DHW heat pump has temperature wise good possibility to perform well, meaning with low power consumption.

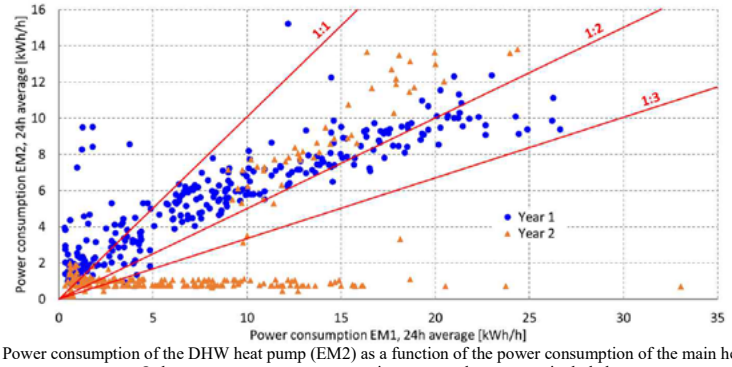

Figure 10 Power consumption of the DHW heat pump (EM2) as a function of the power consumption of the main heat pump (EM1). Only compressor power consumption measured, no pumps included.

Looking at the power consumption of the DHW heat pump (EM2) compared to the power consumption of the main heat pump, see Figure 10, the DHW heat pump (EM2) has too high power consumption. With all heat coming from the subcooler of the main heat pump, in a well-designed system, the ratio would be below 1:3 or at least 1:2 at all time, but mostly significantly lower. This is not the case, the main part of operation is at higher ratios, especially the first year and during the winter the second year. This likely means that the EM2 is heated by the condenser of EM1, causing the lower than necessary Performance Factor seen in Figure 7 and Figure 8. This is possible, circuit and control wise, see green long-dashed lines of Figure 2. Noteworthy is the extreme low ratio in the left side of Figure 10. It is identified that the condenser of the DHW heat pump (EM2) has the possibility, control and circuit wise, to heat its own evaporator, this possible short circuit could be the reason for this extreme operation, see green long-dashed lines in combination with brown dashed lines of Figure 2.

The line of orange rectangles along the x-axis in Figure 10 is likely when the EM2 is focused on producing DHW, meaning the control system is operating correctly. In Figure 11 the DHW production as a function of power consumption of the same heat pump is seen.

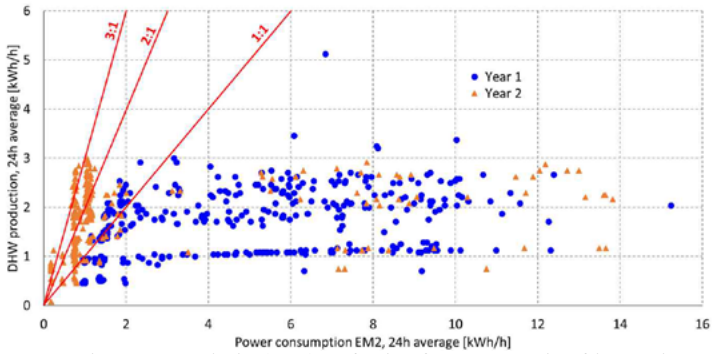

Figure 11 Domestic Hot Water production (DHW) as a function of power consumption of the DHW heat pump (EM2)

It is clear that the DHW heat pump (EM2) is operating in heating mode most of the first year and during the winter of the second year, as the ratio is well below 1:1, meaning extensive unaccounted losses in the DHW system as the only other possible solution. As far from full heating capacity of the main heat pump is not used, see Figure 7, this is not optimal. One possible answer to this poor operation could be found on the nameplate of the main heat pump, it is a chiller with a maximum return temperature of 45°C, meaning the DHW heat pump possibly must aid it at higher heating system temperatures.

According to the nameplate of the DHW heat pump it is also a chiller, not a dedicated heat pump. It has the same maximum return temperature (45°C), meaning about 5-10°C lower than what is necessary to handle legionella temperatures according to Swedish legislation. This means the DHW heat pump continuously is operating outside the envelope stated by the manufacturer, to handle the legionella temperatures, if it does. At the site visit the return DHW circulation temperature was 8°C lower than the legislative requirement, and the cover of the heat pump was removed for simple reset when the machine tripped a high pressure side alarm.

The building used about 15 MWh of DHW per year, including DHW circulation losses, a fraction of the heat supplied (210-290 MWh). The DHW heat pump (EM2) is largely oversized for the purpose, giving it low possibility to handle DHW temperatures accurately.

3.5 The three-port rotary control valve

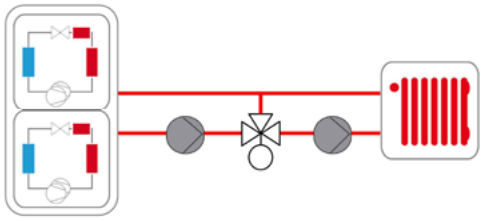

Figure 12 The three-port rotary control valve solution within the heating system, simplification of Figure 2. Pictograms by TU Braunschweig IGS, used with permission within the course of IEA HPT Annex 52

The three-port rotary control valve used between the main heat pump and the heating system, see Figure 12, leads to elevated temperature for the condenser, if not fully open at all time, causing lower Performance Factor, especially at lower load operation, seen in Figure 7 and Figure 8. At the site visit the temperature increased rapidly over the condenser, causing compressor stops after five minutes. Repeated short compressor operating time can cause premature compressor failures and will lead to transient losses [1] that, especially in combination with elevated condenser temperature, will lead to poor performance. The reason for the short compressor operating time is likely that the three-port rotary control valve decreases the working fluid volume for the heat pump to a minimum, by effectively cutting of the heating systems large fluid volume.

This three-port rotary control valve solution is not to be used in a well-designed heat pump system, except for decreasing temperatures to sub heating systems with lower operating temperatures.

3.6 Discussion

The heat pump solution underperforms according to expected performance for a heat pump with an aquifer heat source, heating a state-of-the-art Swedish office building with a low temperature heating system. The unnecessary complexity of the system, with a DHW heat pump in series with the main heat pump and unintuitive circuit layout means it is very difficult to understand when in operation. This was clearly stated by the personnel met at the site visit.

Due to lack of temperature data no relevant uncertainty analysis for the performance factors could be calculated

4 Conclusions

The GSHP solution in this report is complex, with a control system that most likely would need improvements to perform well. The 0.3 MW total heating capacity is almost three-fold the maximum heating demand seen during the two-year measurement period 2012-2014, despite having very cold winter days these years. This means only two of the four compressors in the main heat pump will be used, most of the year there is surplus heating capacity with only one compressor.

The DHW heat pump is seen operating many hours in heating mode, despite its purpose is for DHW. With an unknown change to the control system the second year, made twice, the DHW heat pump heated the heating system significantly less, meaning an overall higher performance factor for the system. Due to system design the DHW heat pump has the ability to heat its own evaporator, it has been identified that it likely does that during the first year. Moreover, the DHW was at times heated by the condenser of the main heat pump, causing lower performance factor, instead of the intention of using the subcooler heat.

A three-port rotary control valve is restricting the flow to the heating system and thus likely elevating the condensing temperatures of the main heat pump. This causes lower performance factors, but also leads to shorter than necessary run time for the compressors, being observed during the site visit. This solution should be avoided in heat pump heating systems. The Seasonal Performance Factor, SPF_{H4} is as low as 2.5 the first year and 2.7 the second year.

The compressors of the heat pump system are not controlled to run actively at cooling operation, the aquifer is then passively supplying the cooling to the building. This means a good potential for high performance factors, but it deteriorated with lower load, suggesting pump management is poor. The pump power

consumption is significantly higher than needed at low cooling demand. The cooling system has regardless high Seasonal Performance Factor, SPF_{C4} was 5.7 the first year and 5.8 the second year.

No temperature data was available; thus no scientifically valid uncertainty analysis was possible to perform. All system boundaries used in the report are the IEA Annex 52 proposal.

Acknowledgements

The support from the Swedish Energy Agency (TERMO research program Grant 45979-1) is gratefully acknowledged. This work is part of the IEA HPT Annex 52, *Long-term performance measurement of GSHP systems serving commercial, institutional and multi-family buildings*.[2].

References

[1] Naicker, S. S. and S. J. Rees.: Performance Analysis of a Large Geothermal Heating and Cooling System. Renewable Energy 122:429–442. https://doi.org/10.1016/j.renene.2018.01.099 (Measurement data available as open access at http://archive.researchdata.leeds.ac.uk/272/). (2018).
[2] IEA HPC.: Annex 52 - Long term performance measurement of GSHP Systems serving commercial, institutional and multi-family buildings . Retrieved Nov. 15, from https://heatpumpingtechnologies.org/annex52/
[3] Gehlin S, Spitler J, 2019, Half-term Results from IEA HPT Annex 52 - Long-term Performance Monitoring of Large GSHP Systems, 13th IEA Heat Pump Conference 2020, Korea
[4] Nordman R, Kleefkens O, Riviere P, Nowak T, Zottl A, Arzano-Daurelle C, Lehmann A, Polyzou O, Karytsas K, Riederer P, Miara M, Lindahl M, Andersson K, Olsson M, 2012, SEasonal PErformance factor and MOnitoring for heat pump systems in the building sector SEPEMO-Build Final report,
[5] Historical temperature data from SMHI. Retrieved Sept. 1, from https://www.smhi.se/data/meteorologi/ladda-ner-meteorologiska-observationer/#param=airtemperatureInstant,stations=all
[6] Spitler, J.D. and S.E.A. Gehlin.: Measured performance of a mixed-use commercial-building ground source heat pump system in Sweden. Energies 2019, 12, 2020; doi:10.3390/en12102020. Open access at: https://www.mdpi.com/1996-1073/12/10/2020 (2019).
[7] Abuasbeh, M., Acuña, J.: ATES System Monitoring Project, First Measurement and Performance Evaluation: case study in Sweden. IGSHPA Research Track 2018, Stockholm, Sweden, September 18th 2018. (2018).

13th IEA Heat Pump Conference 2020

13th IEA Heat Pump Conference
April 26-29, 2021 Jeju, Korea

Design of a gas-driven hybrid adsorption heat pump coupled to geothermal heat exchangers for retrofitting applications

Valeria Palomba[a*], Antonino Bonanno[a], Davide La Rosa[a], Stefan Löwe[b], Ralph Herrmann[b], Andrea Frazzica[a]

[a]Istituto di Tecnologie Avanzate per l'Energia CNR-ITAE, Messina (Italy)
[b]Fahrenheit GmbH, Halle (Germany)

Abstract

The need for retrofitting of residential buildings with energy efficient solutions requires for the development of a wide range of solutions, suitable for different climates and buildings. In the present paper, a concept based on a gas-driven sorption heat pump using geothermal source for evaporation is presented. A dynamic luped-parameter model was implemented in Dymola and used to verify the flexibility of the system in terms of response to variable load and comfort conditions. The outcomes of the activity will be used to propose an improved design of the system.

Selection and/or peer-review under responsibility of the organizers of the 13th IEA Heat Pump Conference 2020.

Keywords: sorpion; geothermal; residential.

1. Introduction

The building heating and cooling sector is accounting for a relevant amount of primary energy consumption in Europe. So far, according to EU, less than 20% of heating and cooling is provided by renewable sources. Heat pumps represent an innovative solution to increase the share of renewables at the building scale, thus participating to the decarbonisation of the heating and cooling sector [1]. In order to make them suitable for different climates, keeping high performance in terms of COP/EER also in severe conditions, the exploitation of geothermal energy as ambient heat source/sink is considered of great interest [2]. In particular, advantages of geothermal heat pumps include high efficiencies (COPs of ground source heat pumps are in the range 3–5 while COPs of air source heat pumps are in the range 2.3–3.5) and low operating costs [2]. The application of ground-source heat pumps was investigated and proven in a wide variety of climates, including European Mediterranean and Continental [3,4], Turkey [5], Iran [6] and China [7], as well as in different building typologies, i.e. residential and commercial [4,8]. However, the exploitability of this resource in the built environment, for retrofitting applications, becomes quite challenging due to both, technical and regulatory constraints that limit the drilling procedures for the ground source heat exchangers (GSHEX) installation.

With this mind, the EU funded GEOFIT [9] project aims at the deployment of innovative geothermal heat pump solutions for retrofitting applications. Particularly, an innovative hybrid geothermal heat pump will be developed, tested and installed in two demo sites. Different hybrid geothermal heat pumps have been proposed, such as a solar-geothermal heat pump able to exploit alternatively the heat from vacuum collectors or the ground [10] or a hybrid configuration with the cooling tower and the ground loops connected together [11,12].

Instead, in the present work, the hybrid solution proposed consists of a hybrid gas-driven hybrid adsorption/electric heat pump Indeed, this combination of thermally and electrically driven HP, despite the lower thermal COP compared to an electrical vapour compression chiller, can be efficiently operated with a smaller size GSHEX. This will make the heat pump more suitable for applications with reduced space availability.

In order to assess the feasibility of such a hybrid solution, a detailed dynamic model was developed in Dymola environment. Adsorption heat pump and gas boiler were modelled by means of TIL Media Library, TIL Suite and self-developed components to match the specific characteristics of the hybrid unit developed. Particular focus was put on the control strategy for enhancing the comfort level achievable by the retrofit of existing systems with the hybrid solution proposed. A first prototype will be developed by Fahrenheit GmbH which will be tested at the CNR ITAE lab subsequently.

2. The GEOFIT sorption solution

The core of the hybrid sorption heat pump developed within GEOFIT is a gas-driven sorption heat pump, whose main components are shown in Figure 1. It is based on the two-modules layout from Fahrenheit GmbH commercial system. Each module consists of an adsorber/desorber and an evaporator/condenser. The desorber is connected through the HTF circuit to the gas boiler that allows the regeneration of the sorption material. At the same time, through the vacuum circuit, the refrigerant flows from the desorber to the condenser, that supplies heat at the temperature level requested for space heating. The adsorber is connected in parallel to the condenser through the HTF circuit. The vacuum circuit allows the flow of the refrigerant from the evaporator to the adsorber. The ground heat exchanger allows the use of the soil as heat source for evaporation. The useful effect delivered to the user is represented by the adsorption heat and condensation heat.

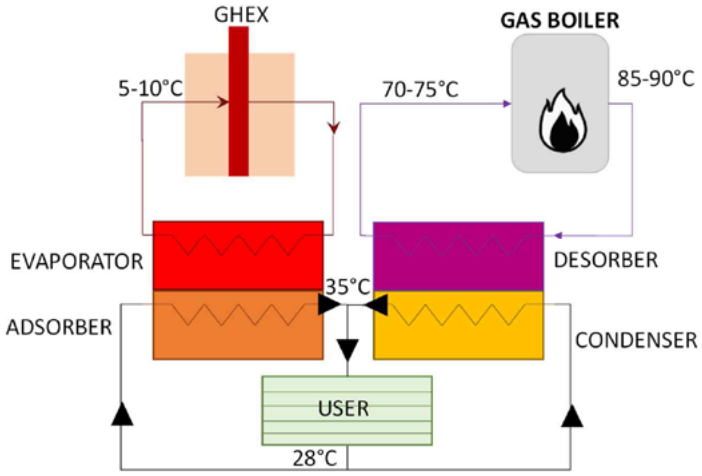

Figure 1: Main layout and thermal levels for GEOFIT hybrid gas-driven heat pump.

The main advantages in the utilization of such thermally-driven heat pumps as retrofitting solutions lies in the possibility of using shallow GSHEXs with a superficial area significantly lower than that needed when the heating system is represented by a vapour compression electrically-driven heat pump.

A schematic of a possible integration of the proposed gas-driven hybrid heat pump is depicted in Figure 2. It is clear that the gas boiler is exploited both to drive the desorption process and to provide domestic hot water (DHW) to the user. The typical distribution system used to increase the heat pump efficiency is a floor heating system, while GHEX is used to provide heat of evaporation in winter and to dump heat of condensation in summer.

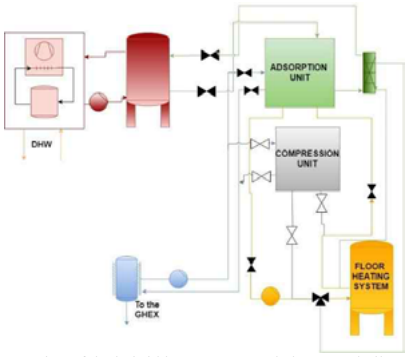

Figure 2: Schematic of the integration of the hybrid heat pump coupled to a gas boiler and the space heating system.

3. The modelling approach

The modelling approach used is schematically shown in Figure 3: Modelica language and Dymola commercial software were chosen as simulation environment. The main reasons for such a choice are the possibility of creating acausal and easily reusable models that, thanks to the FMU functionality of Dymola, can be easily exchanged and integrated in other simulation environments[13,14]. In order to model the refrigerant, the Heat Transfer Fluid (HTF) and the main components of the system, the commercial libraries included in TIL Suite were employed. Correspondently, the same structure as for components already included in the libraries, based on a cell level and a component level was employed also for the self-developed models. In particular, standard models based on liquid cells were employed to model the heat exchanger and heat transfer correlations, whereas self-developed model were used for the sorption equilibrium and the vapour/liquid control volume of the evaporator/condenser. The gas boiler was modelled considering a constant thermal power and an efficiency variable with part load and return temperature. All the components are properly managed thanks to specifically developed controls. The main equations of the model are presented in Table 1, while for a more detailed description of the Dymola model for the sorption unit, the reader is referred to [15].

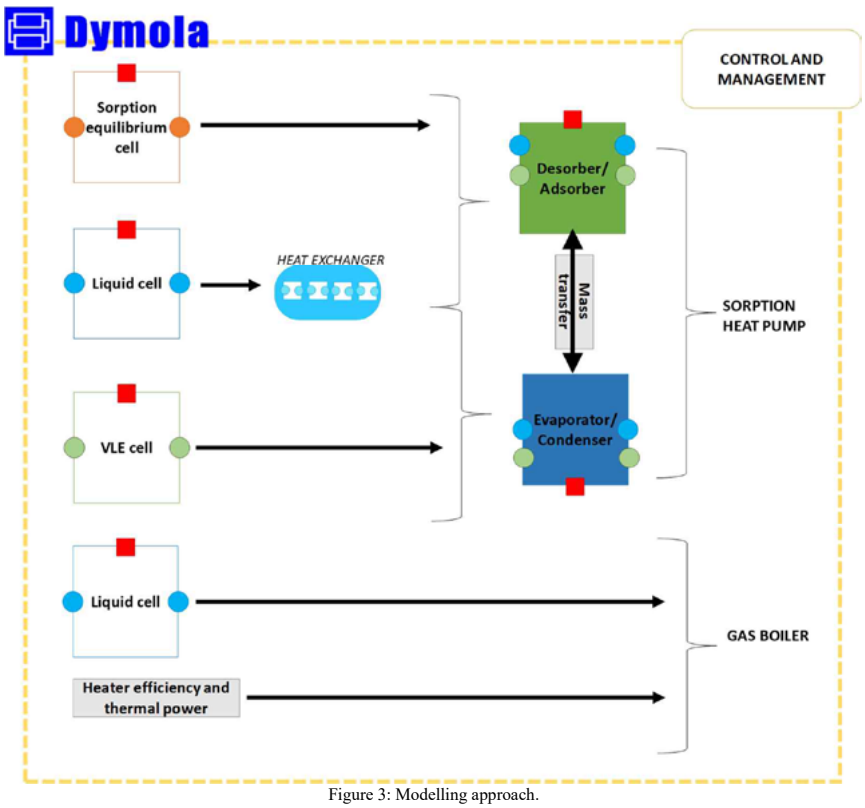

Figure 3: Modelling approach.

4. System control and management

In order to give indications on the best management strategy for the hybrid heat pumps and its integration in retrofitted systems, different controls were implemented and evaluated. In particular, three possible options for controlling the system were considered:

a. Variable flow rate of the pumps according to part load;
b. Step variation of the cycle time of the adsorption unit using the load requested by the user as target variable;
c. Step variation of the cycle time of the adsorption unit using the temperature in the user circuit as target variable.

The models for such components were developed in Dymola using existing components from Modelica Standard Library.

Since the main goal for the system under the GEOFIT activity here presented is the retrofitting of existing heating systems in different climates, two key elements play a particularly significant role:

1. the design of components, that must be as compact as possible;
2. the possibility of ensuring the same level of comfort and a flexible operation, in terms of adaptivity to the load of the building.

The first goal can be achieved thanks to the use of zeolite/water working pair, applying the patented crystallization technique developed by Fahrenheit [16], that has a significant higher power density when compared to standard silica gel/water systems on the market [17].

Instead, the second goal was the focus of the numerical activity here presented. Two key aspects were evaluated: the possibility of delivering a constant temperature to the user under different climatic conditions and the proper management of the sorption unit to be adaptable to user load.

Table 1: List of main equations used for the model implementation.

Component		Equation	
Adsorber	Mass balance sorbent cell	$\dot{m}_{ref} = \dot{m}_{evap} + \dot{m}_{cond}$	(1)
	Energy balance sorbent cell	$\left(m_{sorb}\, c_{p_{sorb}} + w \cdot m_{sorb}\, c_{p_{ref}}\right)\frac{dT_{sorb}}{dt} = \dot{Q}_{fbw} + \dot{m}_{ref}\, h_{ads} - m_{sorb}\, c_{p_{sorb}}\, T_{sorb}\, \frac{dw}{dt}$	(2)
	Mass balance adsorber HEX	$0 = \dot{m}_{in} + \dot{m}_{out}$	(3)
	Energy balance adsorber HEX	$m_{fluid}\, c_{p_{fluid}}\frac{dT_{fluid}}{dt} = \dot{m}_{fluid}\, c_{p_{fluid}}\left(T_{fluid_{in}} - T_{fluid_{out}}\right) + \dot{Q}_{fbw}$	(4)
	Heat transfer sorbent/HEX	$\dot{Q}_{fbw} = (\alpha S)_{ads}\,(T_{sorb} - T_{fluid})$	(5)
	Sorption equilibrium	$w = w_0 \exp(-bA)$	(6)
		$A = -RT_{sorb} \log\frac{p_{ads}}{p_{sat}}$	(7)
Vapor Liquid Equilibrium (VLE) volume evaporator/ condenser	Mass balance	$\frac{dm}{dt} = \dot{m}_v + \dot{m}_l$	(8)
	Energy balance	$\frac{dU}{dt} = \dot{H}_v + \dot{H}_l + Q_{fbw}$	(9)
	Mass balance HEX	$0 = \dot{m}_{in} + \dot{m}_{out}$	(10)
	Energy balance HEX	$m_{fluid}\, c_{p_{fluid}}\frac{dT_{fluid}}{dt} = \dot{m}_{fluid}\, c_{p_{fluid}}\left(T_{fluid_{in}} - T_{fluid_{out}}\right) + \dot{Q}_{fbw}$	(11)
	Heat transfer refrigerant/HEX	$\dot{Q}_{fbw} = (\alpha S)_{evap/cond}\,(T_{VLE} - T_{HEX})$	(12)
	Additional equations	$p_{VLE} = p_{sat}\,(T_{VLE})$	(13)
Mass transfer	Mass balance	$\dot{m}_{ref} = \dot{m}_{in} + \dot{m}_{out}$	(14)
	Linear Driving Force	$\dot{m}_{ref} = m_{sorb}\,\frac{dw}{dt} = m_{sorb}\,\beta(w_{eq} - w)$	(15)
	Mass transfer coefficient	$\beta = \frac{15D}{r_{sorb}^2}$	(16)
Gas boiler	Thermal power output	$\dot{Q}_{fbw} = \dot{Q}_{nominal}\,\eta$	(17)
	Efficiency	$\eta = a * T_{w_{in}} + b * T_{w_{in}}{}^2 + c * T_{w_{in}}{}^3 + d * T_{w_{in}}{}^4 - e * \mathrm{PL} + f * \left(T_{w_{in}} * \mathrm{PL}\right) - g * \left(T_{w_{in}}{}^2 * \mathrm{PL}\right) + h$	(18)

5. Results

To evaluate the adaptability of the heat pump to a variable user load, a signal with changing load (between 4 kW and 8 kW) was used, aiming at simulating a variable user demand. The first approach, based on varying the heat transfer fluid flow rate, resulted not robust enough to let the adsorption machine being properly operated. Accordingly, the control strategy based on the variation of adsorption cycle time as a function of user load was implemented. To this aim, a multi-switch control was used, able to switch between different cycle periods as a function of the expected requested power. Clearly, the higher is the power demand the lower is the cycle time, in order to enhance the average heating capacity provided by the adsorption module, whose behaviour is intrinsically discontinuous due to the physics of the adsorption process[18]. This control is not based on a linear variation of the cycle time, but rather a step variation is investigated. To demonstrate the effect of the variable cycle time on the average power, in Figure 4 the output power provided by the adsorption heat pump is showed. The adsorption/desorption cycle time variation is clearly visible. The average heating power provided increases from about 3 kW at 800 s cycle time up to 5 kW for 200 s cycle time.

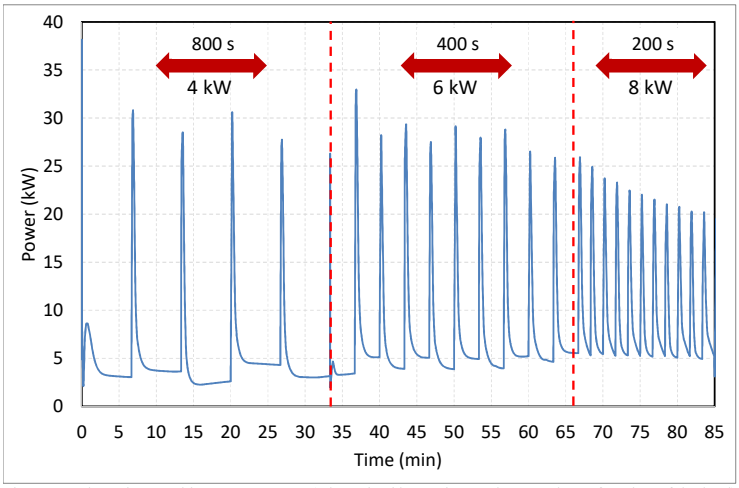

Figure 4: Adsorption machine output power (adsorption/desorption cycle control as a function of the load)

Analysing the temperature of water provided to the user Figure 5) it could be noted that the control works properly when the load is 3 kW and the cycle time is 800 s. Differently, it tends to deviate from the target when the power increases, most probably because the cycle time is reduced too much. This means that, to achieve a proper management, a continuous variation of cycle time according to the measured values of the temperature at each sampling time is needed.

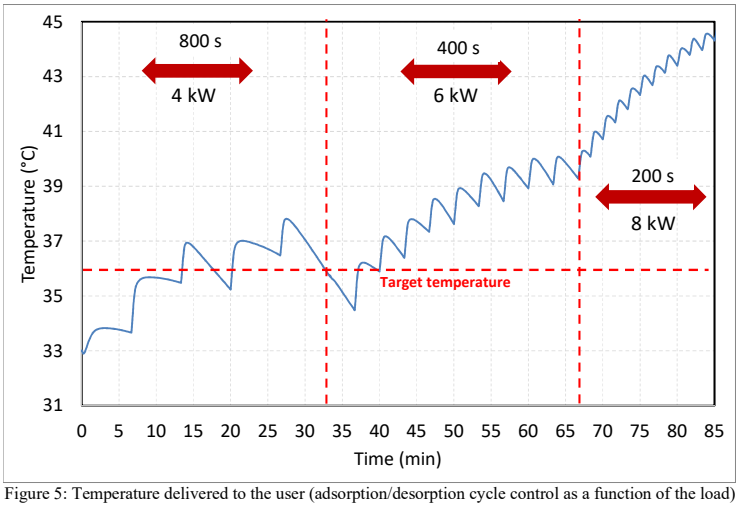

Figure 5: Temperature delivered to the user (adsorption/desorption cycle control as a function of the load)

From such results, it is clear that, to get comfort conditions, it is necessary to use a control that allows a finer tuning in terms of temperatures delivered to the user. Therefore, a second control was developed, that manages in real time the adsorption/desorption cycle time as a function of the temperature delivered to the user. The control compares the signal coming from the T_{user} sensor with the set point (e.g. 35°C); if the measured temperature is lower than the set point, this means that the heating load is higher than the one produced by the adsorption machine, therefore the adsorption/desorption cycle time is reduced. If the measured temperature is higher, than the cycle time is increased, because the requested heating power is decreasing. Compared to the previous case, the cycle time is not imposed a priori, i.e. there is not a predetermined cycle time as a function of the temperature, but rather a user-defined Δt is used for following the user heating demand:

- When the feedback signal $T_{user,measured}$-$T_{user,set}$ is <0, the cycle time is reduced of an amount Δt;

- When the feedback signal $T_{user,measured}$-$T_{user,set}$ is >0, the cycle time is increased of an amount Δt;

Threshold values for minimum and maximum cycle time are imposed as well, to avoid inefficient operation of the unit. Figure 6 reports the power delivered by the adsorption machine for a 30 min operation at variable load with the implemented control. The feedback loop operates changing the cycle time with a Δt of 50 s. The feedback signal is reported in Figure 6 as well. It is possible to notice that the average power output from the sorption heat pump during an overall can be adjusted with this strategy. Furthermore, as confirmed by Figure 7, the proposed approach is able to keep the temperature level delivered to the user close to the target, thus properly operating the adsorption machine. It will be then proposed for the implementation in the prototype to be tested in the lab and then in the demo sites for the GEOFIT project.

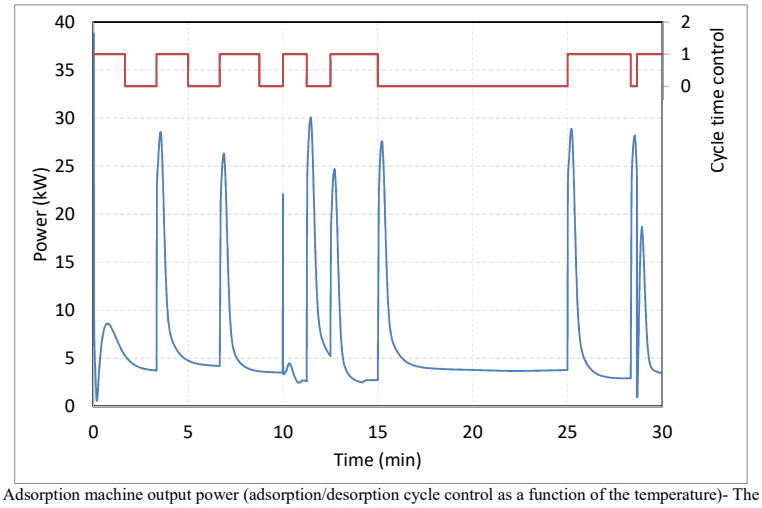

Figure 6: Adsorption machine output power (adsorption/desorption cycle control as a function of the temperature)- The red line indicates the feedback signal based on $T_{user,measured}$-$T_{user,set}$

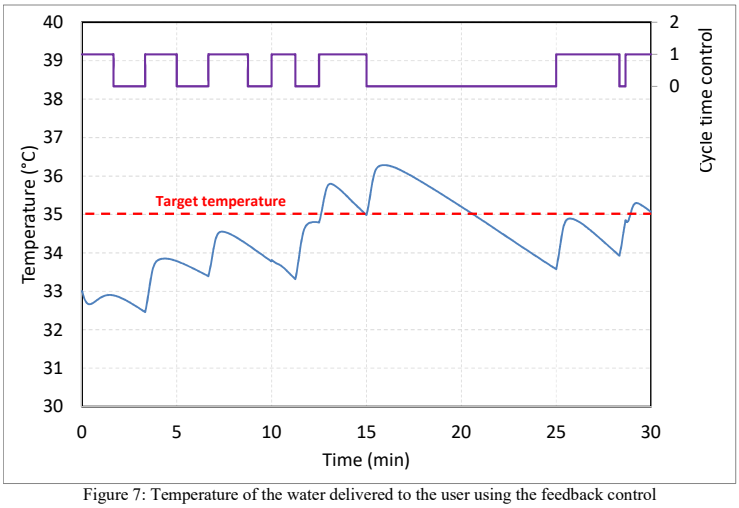

Figure 7: Temperature of the water delivered to the user using the feedback control

6. Conclusions and future activities

The present paper presents the modelling activity of a novel hybrid sorption concept for retrofitting of heating systems in existing buildings, using a gas-driven sorption heat pump and a ground-source HEX as heat

source for evaporation. A dynamic model in Dymola was implemented, including a black-box model of the gas boiler, as well as a detailed adsorption module which comprises heat and mass transfer mode as well as equilibrium data for the given zeolite/water working pair. Particular focus was put on control and management strategies for the system, evaluating the flexibility of the heat pump with variable load and temperature conditions. The best control strategy identified is based on the continuous variation of cycle time according to a feedback control on delivered temperature to the user. As shown in Figure 8, the next steps will include model validation thanks to results from laboratory activity, as well as the definition of an improved design and its adaptation to the pilot sites for the project.

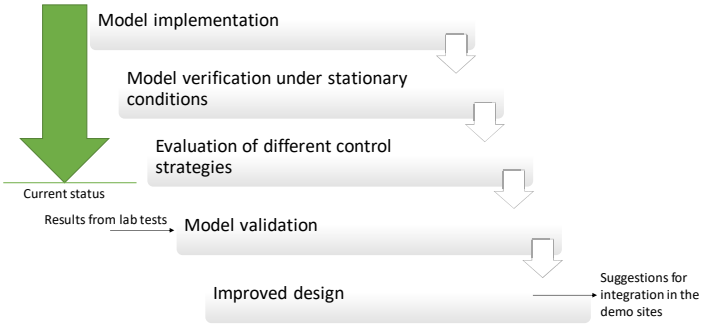

Figure 8: Model development and future steps.

Acknowledgements

This work was funded by the project Geofit: Deployment of novel GEOthermal systems, technologies and tools for energy efficient building retroFITting, which has received funding from the European Commission H2020 Programme under Grant Agreement No. 792210

References

[1] European Commission, COM(2016) 51 final: An EU Strategy on Heating and Cooling | Build Up, (2016). http://www.buildup.eu/en/node/47833 (accessed February 8, 2019).

[2] S.J. Self, B. V. Reddy, M.A. Rosen, Geothermal heat pump systems: Status review and comparison with other heating options, Appl. Energy. 101 (2013) 341–348. doi:10.1016/J.APENERGY.2012.01.048.

[3] D. Antonijevic, M. Komatina, Sustainable sub-geothermal heat pump heating in Serbia, Renew. Sustain. Energy Rev. 15 (2011) 3534–3538. doi:10.1016/J.RSER.2011.05.008.

[4] B. Morrone, G. Coppola, V. Raucci, Energy and economic savings using geothermal heat pumps in different climates, Energy Convers. Manag. 88 (2014) 189–198. doi:10.1016/J.ENCONMAN.2014.08.007.

[5] A. Cetin, Y.K. Kadioglu, H. Paksoy, Underground thermal heat storage and ground source heat pump activities in Turkey, Sol. Energy. (2019). doi:10.1016/J.SOLENER.2018.12.055.

[6] H. Yousefi, H. Ármannsson, S. Roumi, S. Tabasi, H. Mansoori, M. Hosseinzadeh, Feasibility study and economical evaluations of geothermal heat pumps in Iran, Geothermics. 72 (2018) 64–73. doi:10.1016/J.GEOTHERMICS.2017.10.017.

[7] Y. Chang, Y. Gu, L. Zhang, C. Wu, L. Liang, Energy and environmental implications of using geothermal heat pumps in buildings: An example from north China, J. Clean. Prod. 167 (2017) 484–492. doi:10.1016/J.JCLEPRO.2017.08.199.

[8] J. Molavi, J. McDaniel, A Review of the Benefits of Geothermal Heat Pump Systems in Retail Buildings, Procedia Eng. 145 (2016) 1135–1143. doi:10.1016/J.PROENG.2016.04.147.

[9] Geofit project, (n.d.). http://geofit-project.eu/.

[10] J. Choi, B. Kang, H. Cho, Performance comparison between R22 and R744 solar-geothermal hybrid

heat pumps according to heat source conditions, Renew. Energy. 71 (2014) 414–424. doi:10.1016/J.RENENE.2014.05.057.
[11] D.P. Zurmuhl, M.Z. Lukawski, G.A. Aguirre, W.R. Law, G.P. Schnaars, K.F. Beckers, C.L. Anderson, J.W. Tester, Hybrid Geothermal Heat Pumps for Cooling Telecommunications Data Centers, Energy Build. (2019). doi:10.1016/J.ENBUILD.2019.01.042.
[12] L.I. Lubis, M. Kanoglu, I. Dincer, M.A. Rosen, Thermodynamic analysis of a hybrid geothermal heat pump system, Geothermics. 40 (2011) 233–238. doi:10.1016/J.GEOTHERMICS.2011.06.004.
[13] P.A. Fritzson, Introduction to Modeling and Simulation of Technical and Physical Systems with Modelica by Fritzson, Peter A., John Wiley & Sons, Inc, Hoboken, New Jersey, 2011. http://www.amazon.de/Introduction-Simulation-Technical-Sep-30-2011-Paperback/dp/B009KJBU2O/ref=sr_1_1?s=books&ie=UTF8&qid=1376394696&sr=1-1&keywords=fritzson+2011.
[14] Modelica Association, Functional Mock-up Interface, (n.d.). https://fmi-standard.org/ (accessed July 30, 2019).
[15] V. Palomba, E. Varvagiannis, S. Karellas, A. Frazzica, V. Palomba, E. Varvagiannis, S. Karellas, A. Frazzica, Hybrid Adsorption-Compression Systems for Air Conditioning in Efficient Buildings: Design through Validated Dynamic Models, Energies. 12 (2019) 1161. doi:10.3390/en12061161.
[16] Fahrenheit zeolite products, (n.d.). https://fahrenheit.cool/en/zeolite-technology/.
[17] S. Vasta, V. Brancato, D. La Rosa, V. Palomba, G. Restuccia, A. Sapienza, A. Frazzica, S. Vasta, V. Brancato, D. La Rosa, V. Palomba, G. Restuccia, A. Sapienza, A. Frazzica, Adsorption Heat Storage: State-of-the-Art and Future Perspectives, Nanomaterials. 8 (2018) 522. doi:10.3390/nano8070522.
[18] A. Sapienza, V. Palomba, G. Gullì, A. Frazzica, S. Vasta, A new management strategy based on the reallocation of ads-/desorption times: Experimental operation of a full-scale 3 beds adsorption chiller, Appl. Energy. 205 (2017) 1081–1090. doi:10.1016/j.apenergy.2017.08.036.